ABSTRACT

A THREE STAGE LARGE DYNAMIC RANGE AUTOMATIC TRANSIMPEDANCE CONTROL AMPLIFIER

by
Karim Joseph Sikias

Long haul fiber optic communication systems require extremely sensitive, low noise amplification of the weak photo diode currents generated by the received light power. Two types of amplifiers have been used for this application: a high input impedance integrating amplifier/differentiating equalizer combination or a transimpedance amplifier. Optical receivers designed with integrating amplifiers exhibit severe low frequency drift and overload problems and are not generally used in wide dynamic range receiver design. This thesis will describe an extremely wide dynamic range transimpedance amplifier incorporating unique methods to maintain stability, wide bandwidth low pulse width distortion during overload conditions.

A THREE STAGE LARGE DYNAMIC RANGE AUTOMATIC TRANSIMPEDANCE CONTROL AMPLIFIER

by
Karim Joseph Sikias

A Thesis
Submitted to the Faculty of
New Jersey Institute of Technology
in Partial Fulfillment of the Requirements for the Degree of
Master of Science in Electrical Engineering

Department of Electrical and Computer Engineering

January 1995

Blank Page

APPROVAL PAGE

A THREE STAGE LARGE DYNAMIC RANGE AUTOMATIC TRANSIMPEDANCE CONTROL AMPLIFIER

Karim Joseph Sikias

Dr. Kenneth Sohn, Thesis Advisor | Date
Acting Chairman of Electrical and Computer Engineering, NJIT

Dr. Edip Niver, Committee Member | Date
Associate Professor of Electrical and Computer Engineering, NJIT

Dr. Haim Grebel, Committee Member | Date
Associate Professor of Electrical and Computer Engineering, NJIT

BIOGRAPHICAL SKETCH

Author: Karim Joseph Sikias

Degree: Master of Science in Electrical Engineering

Date: January 1995

Undergraduate and Graduate Education:

- Master of Science in Electrical Engineering,
  New Jersey Institute of Technology,
  Newark, New Jersey, 1995

- Bachelor of Science in Electrical Engineering,
  New Jersey Institute of Technology,
  Newark, New Jersey, 1992

Major: Electrical Engineering

This thesis is dedicated to
my parents
Joseph and Yolande

ACKNOWLEDGMENT

The author wishes to express his sincere gratitude to his advisor, Professor Kenneth Sohn, for his guidance, friendship, and moral support throughout this research.

Special thanks to Professors Edip Niver and Haim Grebel for serving as members of the committee and for providing valuable comments and suggestions for this thesis.

The author is grateful to ANADIGICS, Inc. for funding of the research, through the Manager of the Fiber Optics ICs, Tim Laverick.

And finally, the author appreciates the timely help from ANADIGICS' assembly area members, including: Athena Iaonnou, Linda Raspa, and Debbie Yuhas.

TABLE OF CONTENTS

LIST OF TABLES

LIST OF FIGURES

LIST OF FIGURES
(Continued)

Figure **Page**

CHAPTER 1

INTRODUCTION

1.1 Transimpedance Amplifier (TIA) Overview/Background

A transimpedance amplifier is configured as shown in Figure 1 at the bottom with a photo detector connected to the input node. The purpose of the TIA is to convert the small current generated by the photo diode into an amplified, replicated output voltage, and hence the transfer function is a current to voltage conversion (transimpedance) V/I. The constitution of a good TIA is high sensitivity (η), wide dynamic range and wide bandwidth (B). Also shown is the simplified equivalent circuit with the photo diode replaced by an equivalent capacitance (CT), which represents the diode depletion capacitance (C_d) plus the TIA input FET capacitance ($C_{gs} + C_{gd}$), plus stray capacitance (C_{stray});

$$CT = C_d + C_{gs} + C_{gd} + C_{stray}.$$

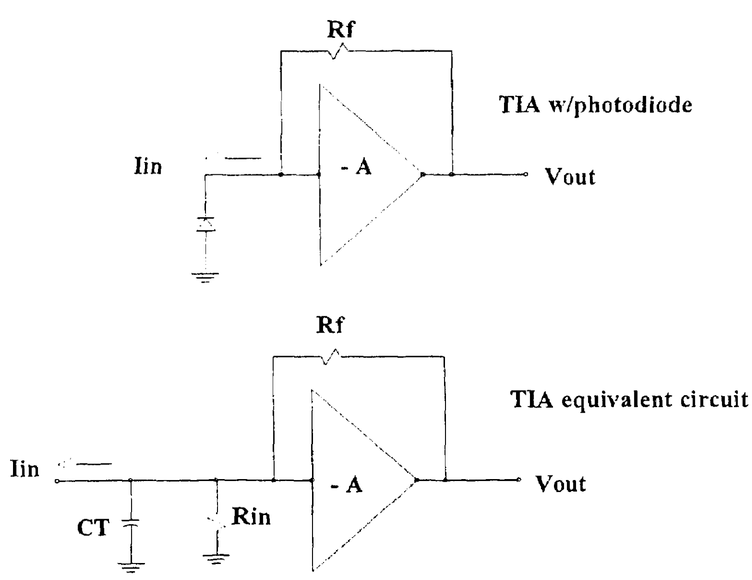

Figure 1 Transimpedance Amplifier Configuration

The dominant pole is formed by the CT in Parallel with the TIA input resistance R_{IN}. With the assumption that the amplifier (-A) has wide open loop bandwidth, then the input resistance Rin is equal to:

$$R_{IN} = \frac{R_f}{1 + Av} \quad (1)$$

The equivalent photo diode series resistance is not shown since it is assumed to be much higher than the input resistance of the TIA (R_{IN} is typically 30 to 500 Ω and PIN diode series resistance is typically larger than 5 KΩ) and hence the equivalent input impedance looking into the TIA is given by:

$$Zin = \frac{1}{1/Rin + j\omega C_T} = \frac{1}{\frac{1 + Av}{R_f} + j\omega C_T} \quad (2)$$

Conversion of input current to output voltage is more efficient when the open loop gain A_V is made as large as possible (1) since a high impedance current source (photo diode) provides maximum power transfer when loaded with a short circuit.

From equation (2) the -3dB Bandwidth B can be shown as

$$B = \frac{Av}{2\pi R_f(C_{gs} + C_{gd} + C_d + AC_f)}$$

and can be simplified to be

$$B = \frac{Av}{2\pi R_f C_T} \quad (3)$$

From the equations above it is apparent that the TIA design is one of compromise and optimization, since sensitivity (a low noise receiver has high sensitivity) is proportional to, and the bandwidth is inversely proportional to the value of R_f . Also since it is economically desirable to use the same optical receiver components for links which may have a high average received power (i.e. a Local Area Network where transmission distances are short and hence received powers are as high as (+3 dBm) These inherent tradeoffs will be discussed later .

1.2 Noise

The sensitivity of a digital optical receiver is a measure of the lowest level of optical information that can be discriminated above the transmission system noise level. In real economic terms, sensitivity is one factor that determines the distance between optical receivers and hence the number of repeaters (cost) needed for a given transmission distance. For example, current optical fiber technology produces fiber with attenuation of < 0.2 dB/km, so for every increase in sensitivity of 0.2 dB, the repeater spacing can be increased by 1km.

In a TIA, the input referred noise current is the figure of merit since the transfer function is one of current to voltage conversion ($V_{out} = I_{in} * R_f$). The dominant sources of noise are the input FET, the input stage load FET, and the feedback resistor R_f, since they all contribute noise close to the input node and will pass through the highest amount of gain. The input referred (thermal) noise generated by the feedback resistor R_f can be shown as

$$\overline{I_{Rf}^2} = \frac{4kTB}{R_f} \tag{4}$$

where:

- B is the bandwidth of an ideal low pass noise spectrum truncation filter

- T is temperature

- k is Boltzman's constant.

In a well designed TIA the dominant source of FET input referred noise is generated by the input FET [1]. To minimize noise and maximize sensitivity, the size of the input FET is chosen so that its $C_{gs} + C_{gd}$ is equal to the photo diode capacitance C_d [2]. From [1] [3] the noise contributions of the input stage load FET in a practical design will only be about one sixth that of the input FET and then its noise can be shown as

$$\overline{I^2_{INFET}} = \frac{(4kT\Gamma)8\pi B^3 C_d}{3F_t} \tag{5}$$

where:

- $\Gamma = 1.3$ is a GaAs excess noise factor

- F_t is the cutoff frequency of the input FET

Assuming that all noise sources are gaussian (even noise sources that are non-gaussian will only contribute about 1dB of error), the sensitivity η (dBm) can be calculated from input referred current i_n by:

$$\eta = 10\log_{10}\left[1000\frac{6.5 \times i_n}{R}\right] \text{ assuming } 10^{-10} \text{ Bit Error Rate} \tag{6}$$

where R is the responsivity of the photodetector (A/W)

CHAPTER 2

OPTICAL COMMUNICATIONS

Lightwave technology has revolutionized the transmission of analog and digital information. Because the light output intensity from a semiconductor laser is linearly proportional to the injected current, and the current generated in a photodetector is linearly proportional to the incident optical intensity, analog information is transmitted as modulation of the optical intensity. The lightwave system is analogous to a linear electrical link, where current or voltage translates linearly into optical intensity. High-speed semiconductor lasers and photodetectors enable intensity-modulation bandwidths greater than 10 GHz. Hence, a wide variety of radio frequency (RF) and microwave applications have been developed [5].

Converting microwaves into intensity-modulated (IM) light allows the use of optical fiber for transmission in place of bulky inflexible coaxial cable or microwave waveguide. Since the fiber attenuation is 0.2-0.4 dB/km, compared with several decibels per meter for waveguide, entirely new applications and architectures are possible. In addition, the signal is confined tightly to the core of single-mode fiber, where it is immune to electromagnetic interference, cross talk, or spectral regulatory control.

To achieve these advantages, several limitations must be overcome. The conversion of current to light intensity must be linear. Several nonlinear mechanisms must be avoided by proper laser design or by the use of various linearization techniques. Also, because the photon energy is much larger than in the microwave systems, the system fidelity is limited by quantum or shot noise. In this thesis the discussion will be limited to digital systems since the TIA will be used in a digital long-distance fiber systems.

When the first laser was demonstrated in 1960, numerous applications of this magnificent new tool were anticipated. Some predicted that the laser beams would transmit messages through the air at high data rates between distant stations. Although laser beams can indeed travel through the atmosphere, too many problems prevent this scheme form becoming practical. Included in the objections are the need for line-of-sight paths and the unpredictability of transmission through an atmosphere where weather variations randomly change path losses. Guided paths using optical fibers offer the only practical means of optical transmission over long distances.

Long-distance fiber systems tend to have the following operational characteristics:

- They are more than 10 km long
- Transmit digital signals (rather than analog)
- Operate at data rates above a few tens of megabits per second.

Figure 2 illustrates the basic structure of a generalized long-distance fiber optic link. Each of the components will be described in the following paragraphs.

The bandwidth of the transmitting and receiving circuits (including the light source and photodetector) limits the achievable system data rate. The bandwidth of the fiber decreases with its length, so that the fiber itself limits the rate-length product (a figure of merit which is the product of the system data rate and its length). The losses in the system, including those in the fiber, also limit the path length.

The first efficient fiber appeared in 1970, having a loss of 20 dB/km. Just 7 years

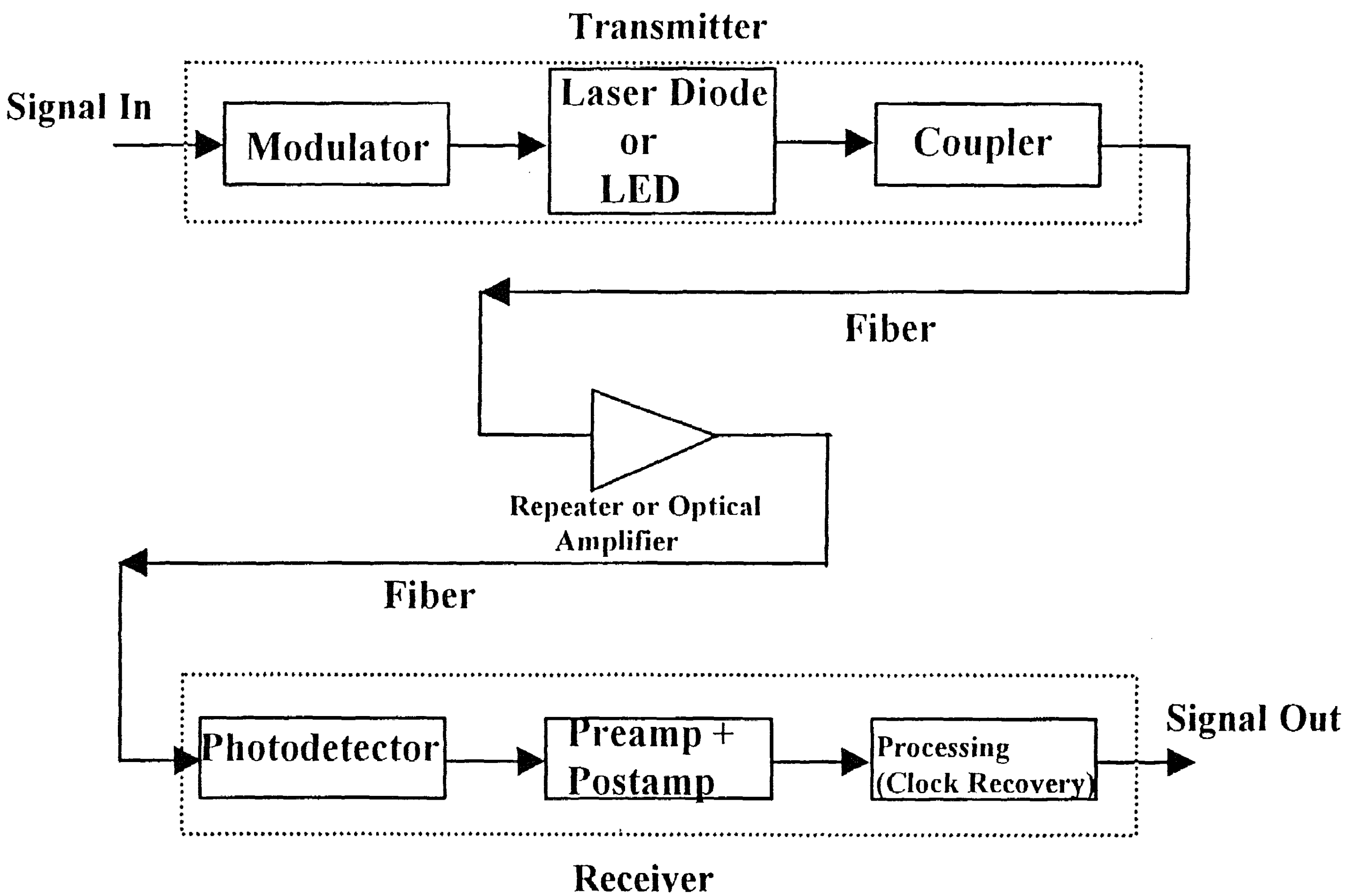

Figure 2 Typical Fiber Optics Communication System

later the first large-scale application, a link between two telephone exchanges in Chicago, was constructed. By this time the loss had been reduced to around 3dB/km. The digital technology used could accommodate a rate of 45 Mb/s over an unrepeated length of 10 km and a total length of over 60 km with repeaters. The unrepeated rate-length product for this initial system was a modes 0.5 Gb/s x km. As fiber technology advanced, this figure steadily increased. Unrepeatered rate-length products have improved to 500 Gb/s x km (e.g., 8 Gb/s over a path of 60 km) an beyond. Allowing repeaters and/or optical amplifiers increases the net rate-length product considerably [13].

All fibers used for long-distance communications are made of silica glass and allow only a single mode of propagation. The silica is doped with other materials to produce the required refractive index variations for the fiber core and cladding. The important fiber characteristics that limit system performance are its loss and its bandwidth. The loss limits the length of the link and the bandwidth limits the data rate.

Figure 3 shows the loss characteristics of single-mode silica fibers at the wavelengths of lowest attenuation. As indicated in the figure, there are three possible windows of operation. In the first window (around 820 nm), the loss is typically 3 dB/km. This is too high for long systems. In the second window (near 1300 nm), the loss is about 0.5 dB/km. In addition, the fiber bandwidth quite high because of low pulse distortion at this wavelength. The second window is a reasonable operating wavelength for high-capacity, long distance systems. At 1550 nm (the third window) the loss is lowest, about 0.25 dB/km. This characteristic makes 1550 nm the optimum choice for the very longest links.

Dispersion refers to the spreading of a pulse as it travels along a single-mode fiber. It is

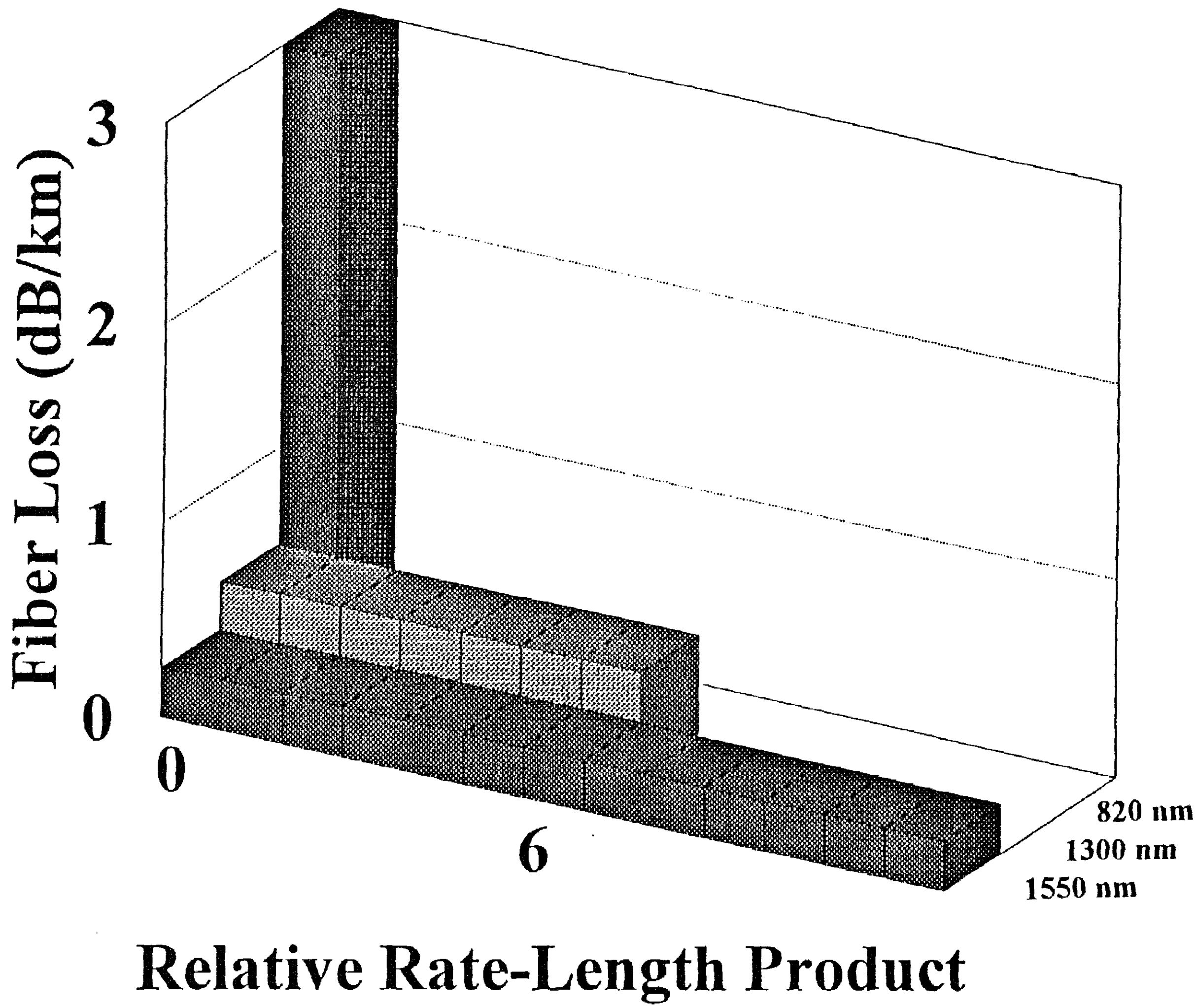

Figure 3 Loss Characteristics of Single Mode Fiber

due to material and waveguide effects. This spreading creates intersymbol interference if allowed to exceed about 70% of the original pulse width, causing receiver errors. The dispersion factor M is usually given in units of picoseconds of pulse spread per nanometer of spectral width of the light source and per kilometer of length of fiber.

In the range from 1200 to 1600 nm, the dispersion curve for silica can be approximated by the expression

$$M = \frac{M_0}{4}\left(\lambda - \frac{\lambda_0^4}{\lambda^3}\right) \tag{7}$$

Where

- λ is the operating wavelength
- λ_0 is the zero dispersion wavelength
- M_0 is the slope at the dispersion wavelength.

M_0 is approximately 0.095 ps/(nm^2 x km). The pulse spread for a path length L, using a light source whose spectral width is $\Delta\lambda$, is then

$$\Delta\iota = ML\Delta\lambda \tag{8}$$

The zero dispersion wavelength, close to 1300 nm for silica fibers, makes this wavelength attractive for high-capacity links. The dispersion at 1550 nm is typically close to 20 ps/(nm x km). This is a moderate amount of dispersion. If a proposed 1550 nm system is bandwidth limited because of this spread, several alternatives are available. One solution is to use dispersion-shifted fiber, which is a special fiber with refractive index profile designed to shift the zero dispersion wavelength from 1300 nm to 1550 nm.

Because of high loss, (from Figure 3) the first window can be used only for moderate lengths (around 10 km). Because of high dispersion, data rates are also limited in this region. In the second window, nearly zero dispersion allows high-rate transmission, but the losses limit the distance that can be covered (typically around 50 km). In the third window, the loss is about half the 1300 nm attenuation so that twice as much distance can be covered. Dispersion-shifted fiber allows the same high rates as does 1300 nm operation. Repeaters and amplifiers extend the useful distance of fiber links well beyond the distances list here.

At the transmitter side we start with the modulator. A digital electrical signal modulates the light source. The driver circuit must be fast enough to operate at the system bit rate. As bit rates increase into the multigigabit per second range, this becomes increasingly difficult. Modulation can be done in the optical domain at very high speeds. In this case, the modulator follows the laser diode rather than preceding it. External modulation is usually accomplished using integrated-optic structures.

Laser diodes or light-emitting diodes (LEDs) supply the optical carrier waves for most fiber links. LEDs cannot operate at speeds in the gigabit range, but laser diodes can. For this reason, laser diodes are normally required for high-rate, long-distance links. Laser diodes can be modulated at frequencies beyond 40 GHz.

Laser diodes emitting in the second and third fiber transmission windows are semiconductor heterojunctions made of InGaAsP. The exact emission wavelength is primarily determined by the proportions of the constituent atoms. Output powers are commonly on the order of a few milliwatts. Typical laser diode spectral widths are between 1 and 5 nm when operating in more than one longitudinal mode. Single-mode laser diodes can have spectral widths of just a few tenths of a nanometer. As predicted by Eq. (8), narrow-spectral-width emitters minimize pulse spreading. Minimizing pulse spreading increases the fiber bandwidth and its data capacity.

The light emitted from the diode must be coupled as efficiently as possible into the fiber. Because the beam pattern emitted by a laser diode does not perfectly match the pattern of light propagating in the fiber, there is an inevitable mismatch loss. Good coupler designs, sometimes using miniature lenses, reduce this loss to about 3 dB when feeding a single-mode fiber.

Connections between fibers and between the fiber and other components occur at numerous points in a long-distance link. Because there may be many splices in a long system, the loss of each one must be small. Fusion splices with an average loss of no more than 0.05 dB are often specified. Mechanical splices are also suitable. They often involve epoxy for fixing the connection. Connectors are used where remateable connections are required. Good fiber connectors introduce losses of just a few tenths of a decibel.

Many fiber links are loss limited. One cause is the limited power available from the typical laser diode, which (together with the losses in the fiber and the other system components) restricts the length of fiber that can be used. The fiber optic amplifier increases the power level of the signal beam without conversion to the electrical domain. For example, gains of 30 dB are attainable at 1550 nm using the erbium-doped fiber amplifier (EDFA). As indicated in Figure 2, there are a number of possible locations for optical amplifiers in a system. An optical amplifier just following the transmitter increases the optical power traveling down the fiber. Amplifiers along the fiber path continually keep the power levels above the system noise. An amplifier located at the fiber end acts as a receiver preamplifier, enhancing its sensitivity. Many amplifiers can be placed in a fiber network, extending the total length to thousands of kilometers.

The repeater is a regenerator that detects the optical signal by converting it into electrical form. it then determines the content of the pulse stream and uses this information to generate a new optical signal and launch this improved pulse train into the fiber. The new optical pulse stream is identical to the one originally transmitted. The regenerated pulses are restored to their original shape and power level by the repeater. Many repeaters may be placed in a fiber network, extending the total path length to thousands of kilometers. The advantage of optical amplifier over the regenerator is its lower cost and improved efficiency. The greater cost of the regenerator arises from the complexity of conversion between the optical and electrical domains. The regenerator does have the advantage of restoring the signal pulse shape, which increases the system bandwidth.

On the receiver side we have the photodetector which is a device that converts optical beam into an electrical current. In fiber receivers, the most commonly used photodetectors are semiconductor pin photodiodes and avalanche photodiodes (APD). Important detector characteristics are speed of response, spectral response, internal gain, and noise. Because avalanche photodiodes have internal gain, they are preferred for highly sensitive receivers. Both Ge and InGaAs photodiodes respond in the preferred second and third fiber windows. InGaAs performs better at low signal levels because it has smaller values of dark current (that is, it is less noisy).

The current produced by a photodetector in response to incident optical power P is

$$I = M\eta eP/hf \tag{9}$$

Where

- M is the detector's gain (in case of an APD)
- η is its quantum efficiency (close to 0.9 for good photodiodes)
- h is Planck's constant (6.63×10^{-34} Js)
- e is the magnitude of the charge on an electron (1.6×10^{-19})
- and f is the optical frequency.

For pin photodiodes (M = 1), typical responses are on the order of 0.5 to 0.9 μA/μW.

On the receiver side an electronic amplifier is normally used following the photodetector knowing that at the input of the receiver low power levels are expected. The remainder of the receiver includes such electronic elements as low and band-limiting filters, equalizers, decision-making circuitry, other amplification stages (post-amp), switching networks, digital-to-analog converters, and output devices (this receiver part will be explained in details in chapter 3).

Long-distance fiber links carry in general voice, video, and data information. Therefore messages not already in digital form are first converted. A single voice channel is usually transmitted at a rate of 64,000 bits per second. On the other hand video requires a much higher rate. The rate could be as much as 90 Mb/s or so, but video compression techniques can lower this rate significantly. Fiber systems for the telephone network operate at such high rates that many voice channels can be time-division multiplexed (TDM) onto the same fiber for simultaneous transmission. For example, a fiber operating at a rate 2.3 Gb/s could carry more than 30,000 digitized voice channels [5].

A major part of the fiber system design involves the power budget and bandwidth budget. In any fiber system, component losses (or gains) are normally given in decibels, where the decibel is defined by

$$dB = 10 \log P_2/P_1$$

where P_2 and P_1 are the output and input powers of the component. The decibel describes relative power levels. Similarly, dBm and dBμ describe absolute power levels. They are given by

$$dBm = 10 \log P$$

where P is in milliwatts and

$$dB\mu = 10 \log P$$

where P is in microwatts.

The total system response can be expressed in terms of the rise time for the transmitter t_t, the fiber t_f, and the receiver t_r as follows:

$$t_s \approx \sqrt{t_t^2 + t_f^2 + t_r^2} \qquad (10)$$

On the other hand, the amount of information to be transmitted by the system with bandwidth B can also be expressed in terms of a time constant tb. Table 1 gives t_b in terms of either the bit rate or the bandwidth B for various signal types. If $t_s < t_b$, the system response is considered to be adequate.

Table 1 Rise-Time Estimate For Various Signal Types

Signal	t_b
NRZ	0.7/bit rate
RZ	0.7/2(bit rate)
IM	0.7/2B
PCM	1/(sampling rate)(bits/sample)(B)

Where:

- NRZ (Not Return to Zero) signal

- RZ (Return to Zero) signal

- IM (intensity Modulation) used in Analog systems

- PCM (Pulse-Code Modulation) which is the digital coding and can be coded simply by means of direct detection. For example, in a simple binary pulse code (0 or 1), the only requirement imposed on the receiver is to determine whether a signal is above or below threshold.

Figure 4 gives an example of the difference between an NRZ and RZ signals. The power budget can be estimated by calculating first the minimum optical power P_d that can be detected by a chosen receiver at a given bandwidth and a signal level required by the signal-to-noise ratio (S/N), and second the maximum signal power P_s that can reach the receiver after allowing for all possible system losses. If $P_s > P_d$, the system chosen is

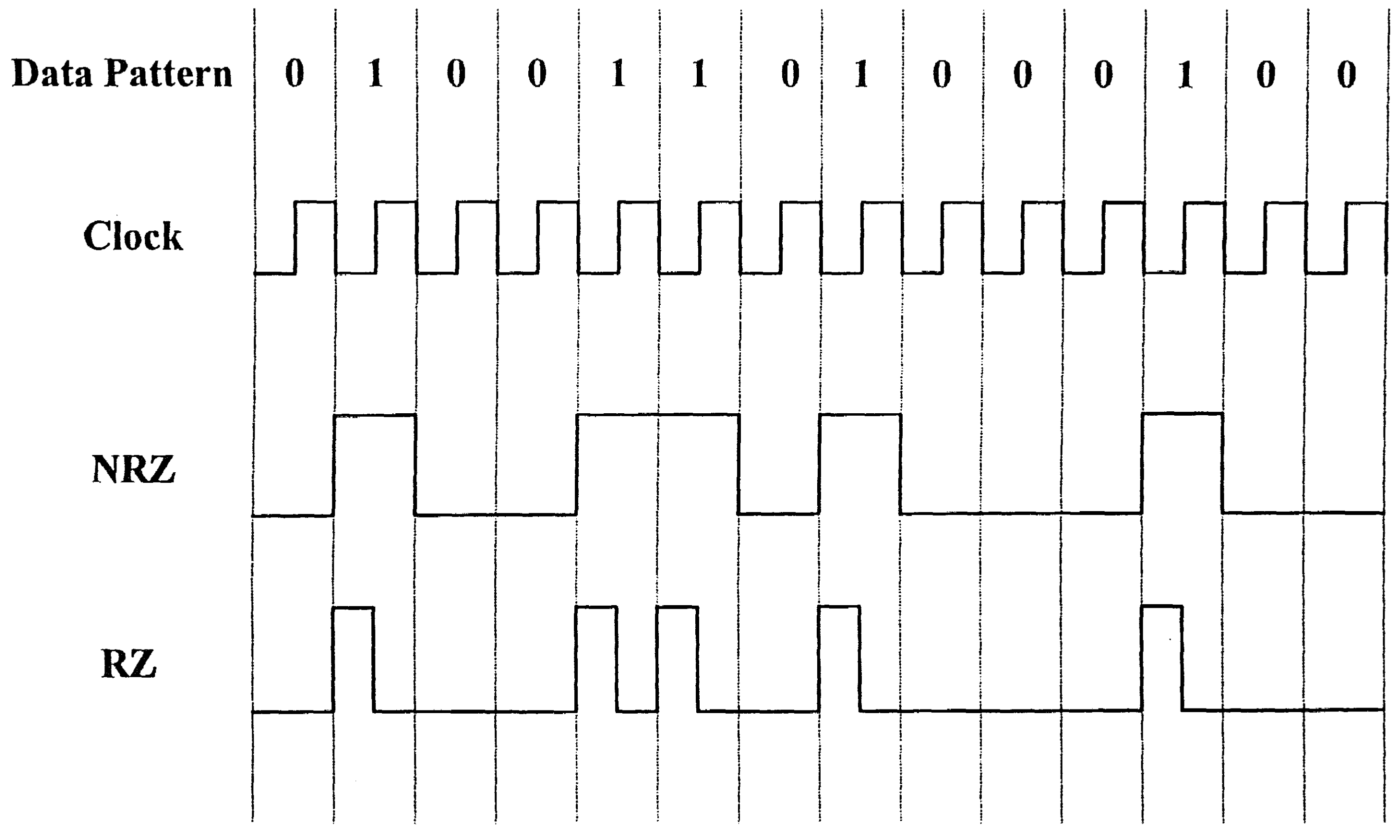

Figure 4 Different Signals

considered to be adequate. The power margin that is the difference between P_s and P_d should be at least 10 dB to allow for component degradation and other unexpected problems (e.g. aging).

The signal-to-noise ratio is a measure of signal quantity. It determines the error rate in a digital network. At the receiver, it is given by

$$\frac{S}{N} = \frac{(M\rho P)^2 R_L}{M^n 2eR_L B(I_D + \rho P) + 4kTB} \tag{11}$$

Where

- P is the received optical power
- ρ is the detector's unamplified responsivity
- M is the detector gain if an APD is used
- n accounts for the excess noise of the APD (usually between 2 and 3)
- B is the receiver's bandwidth
- k is boltzmann's constant ($k = 1.38 \times 10^{-23}$ J/K)
- e is the magnitude of the charge on an electron (1.6×10^{-19} coulomb)
- T is the receiver's temperature in degrees Kelvin
- I_D is the detector's dark current
- and R_L is the resistance of the load resistor that follows the photodetector.

Table 2 gives the results of an analysis that describes a typical digital data link involving one transmitter and one receiver at a bit rate of 20 Mb/s. The length of this link is assume to be 8 km. Over this length, an LED is chosen as the source with an average output of 3 dBm. An APD detector is used in this link and has a time constant of 3ns. The calculated system rise time is about 14 ns, which is well within the time requirement (35ns) specified by the system bandwidth. If a laser source was used instead of the LED, the length of this link can easily be increased by about a factor of 2 or more.

Table 2 Power Budget

	Power Budget	Rise time
Source: LED	3 dBm	6 ns
Signal: NRZ	- 3 dBm	
Fiber: α = 5dB/km	- 40 dB	Dispersion 10 ns
Splicing loss (3)	1.5 dB	
Detector: APD	59 dBm	3 ns
Source/fiber coupling	10 dB	
Fiber/detector coupling	1 dB	
Temperature degradation allowance	1 dB	
Other allowance	5 dB	
System requirement: 40 + 1.5 + 10 + 7 =	58 dB	0.7/20 Mb/s = 35 ns
System performance: 3 - 3 + 59 =	59 dB	$1.11\sqrt{6^2+3^2+10^2} = 13.4$ns

CHAPTER 3

RECEIVERS IN FIBER OPTICS SYSTEMS

The function of optical receiver is to detect the incoming optical signal and to regenerate the transmitted data for further transmission (as in a repeater) or for the receiving end (as in a line terminal). The most critical part of the receiver (see Figure 6) is the photodiode and the following preamplifier, since these two components dictate many of the receiver characteristics as well as its performance. Therefore, a high receiver sensitivity and especially the preamp part of it, is essential to achieve the maximum repeater spacing. This kind of requirement is very critical for long-distance communications especially for submarine systems where we want to minimize as much as we can the total number of repeaters that have to be placed undersea along the link. A wide dynamic range is also critical since it allows flexibility and convenience in system configuration. The ability to accommodate a wide range of optical power levels at the receiver means that the receiver can be used for both short and long-distance systems. This requirement is important in terrestrial communication systems. A wide dynamic range is also important in Local Area Network (LAN) applications, where the transmitting source may be at different distances from the receiver and the transmitting optical power may have to go through a different number of optical couplers and splitters before reaching the receiving end.

The receiver sensitivity is very critical since it is a measure of the minimum optical power level required at the receiver input so that it will operate reliably with a bit error rate less

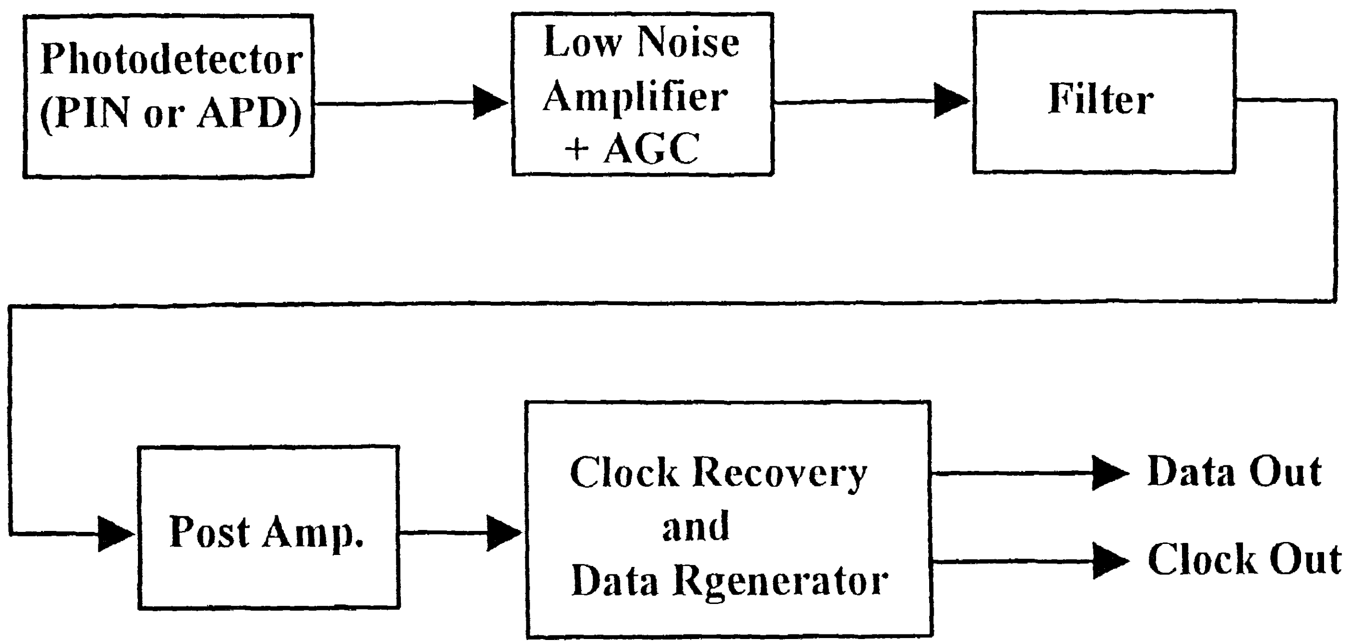

Figure 5 Block Diagram of A Typical Receiver than a desired value [8]. It is often given as the average optical power P required for a bit error rate of 10^{-9} [7].

The receiver sensitivity is a function of both the photodetector and the following preamplifier. Therefore, in order to achieve an excellent performance in receiver sensitivity, both the photodetector and the preamplifier have to be equally good.

The important requirements for the photodetectors are:

1- High quantum efficiency from equation (9)

2- Fast response time

3- Low capacitance since from equation (3) one can see that the input capacitance will effect the bandwidth of the receiver

4- Low dark current

5- and Low avalanche excess noise (if an APD is used)

Materials that are commonly used to fabricate photodetectors are Si, Ge, GaAs, InAs, and InGaAs. In general, indirect bandgap materials, such as Ge and Si, are preferred over direct bandgap materials, primarily because the surface recombination in a direct bandgap material can lead to a substantial loss of carriers as a result of trapping by surface states, without producing photocurrents of significant magnitude. But at the same time Si and Ge have higher capacitance than their counterparts using the III-V material system [18].

Preamplifiers for optical receivers can be classified into two types:

• High impedance (see Figure 6)

• Transimpedance (see Figure 1)

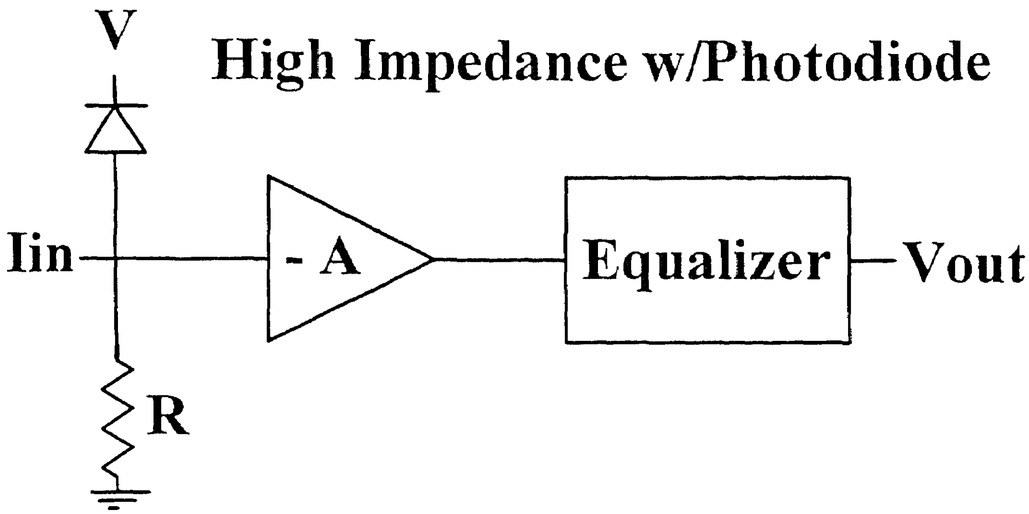

Figure 6 High Impedance Amplifier

The high-impedance receiver amplifier [4], offers the lowest noise level and hence the highest detection sensitivity. However, because of the high load impedance at the front end, the frequency is limited by an RC time constant at the input. Because of this large RC time constant, the high-impedance receiver tends to integrate the detected signal and is also referred to as the integrating front-end design. Thus an equalizer following the preamplifier is necessary to extend the receiver bandwidth out to the desired value. This requirement can introduce complexity into the receiver design where we have to match the pole of the amplifier response with the zero of the equalizing network. Since the amplifier pole can change over the system operating lifetime (e.g. due to changes in device parameters and stray capacitances), any resulting pole-zero mismatch can degrade the receiver sensitivity.

The main drawback of the high-impedance design, is in its limited dynamic range due to the high-input load resistance. In addition, baseline wander effect is more severe due to the integration effect of long strings of ones and zeroes in the input stream of data.

The transimpedance amplifier design is a popular approach in industry to avoid the dynamic range problem[15],[16]. In addition, it is normally designed to take advantage of the negative feedback effect so that the amplifier bandwidth is extended to the desired values. However because of the thermal noise of the feedback resistor, the receiver noise level is higher and the receiver sensitivity is somewhat less than that of a high-impedance design.

The receiver sensitivity degradation of the transimpedance amplifier can be kept somewhat negligible value by keeping the feedback resistance as large as possible [11],[19]. Therefore for a desired bandwidth value, this can be achieved by increasing the amplifier open-loop gain. However, the maximum open-loop gain is somewhat limited by propagation delay and phase shift of the amplifying stages inside the feedback loop. Thus, a certain gain and phase margin is desirable to assure stability and acceptable pulse response. As we can see from equation (4) that the feedback resistance thermal noise of a transimpedance amplifier is normally a significant portion of the total noise.

The receiver preamplifier noise level is often characterized by an input equivalent noise current power $<i_{na}^2>$ at a given operating bit rate [7]. The variation of $<i_{na}^2>$ with bit rate is dependent on whether a bipolar or FET transistor is being used as the front-end amplifying device and whether the preamplifier used is a transimpedance or high-impedance design.

For a FET front-end preamplifier, the input equivalent noise current power is given by [7]

$$<i_{na}^2> = \frac{4kT}{R_f} I_2 B + 2eI_L I_2 B + \frac{4kT\Gamma}{g_m}(2\pi C_T)^2 f_c I_f B^2 + \frac{4kT\Gamma}{g_m}(2\pi C_T)^2 I_3 B^3 \qquad (12)$$

where

- B bit rate,
- R_f feedback resistance in a TIA design (or load resistance in a high-impedance design),
- I_l total leakage current,
- g_m FET transconductance,
- C_T total input capacitance (including photodiode and stray capacitance),
- f_c the 1/f noise corner frequency of the FET,
- Γ numerical constant
- k Boltzmann constant, and
- T absolute temperature.

Γ is a noise factor associated with the channel thermal noise and gate-induced noise in the FET. Typically is 1 for short-channel Si MOSFET's and 1.7 for GaAs MESFET's [12], [20].

The total capacitance C_T is given by

$$C_T = Cds + Cgs + Cgd + Cf \qquad (13)$$

where

- Cds is the photodiode and stray capacitance at the input,
- Cgs gate-to-source capacitance of the FET,
- Cgd gate-to-drain capacitance of the FET,
- Cf feedback resistor capacitance.

From (12), the first noise term is due to the feedback or load resistance which is negligible if high-impedance design is used. The second and third noise terms are from the leakage current and 1/f noise. And finally the last term is due to the channel thermal noise and induced gate noise.

We can see that is desirable to choose a FET with low input capacitance, high tranconductance, low gate leakage current, and low 1/f noise corner frequency. The two known type FET's that are used in the industry are the Si JFET's, and the GaAs MESFET's. It can be observed from [14] that Si junction FET's are useful in the low bitrate range because of their negligible gate leakage current and 1/f noise. However, their low tranconductance and high input capacitance limit their use up to about 50 to 60 Mb/s. On the other hand, the GaAs MESFET's are used in the high bitrate range since they can be fabricated with extremely low capacitance and high transconductance [10]. But their high 1/f noise limit their use below 10 Mb/s.

For a Bipolar front-end preamplifier, the input equivalent noise current power is given by [7]

$$< i_{na}^2 >= \frac{4kT}{R_f} I_2 B + 2eI_b I_2 B + \frac{2eI_c}{g_m^2}(2\pi C_T)^2 I_3 B^3 + 4kTr_{bb'}(2\pi C_{dsf})^2 I_3 B^3 \qquad (14)$$

where

- I_b base bias current
- I_c collector bias current
- $r_{bb'}$ base spreading resistance of the transistor
- g_m transistor transconductance
- C_T the total capacitance defined as $C_T = C_{ds} + C_\pi + C_\mu + C_f$
- C_{dsf} is the capacitance of the detector, stray and feedback capacitance.

For the high-impedance preamplifier design, the first term in (14) due to the load resistance can be neglected. Therefore the input noise power varies as the square of the bit rate until it reaches very high bit rates the last two terms with B^3 become more dominant. For the transimpedance amplifier, the feedback resistor has to be reduced as the bit rate increases in order to accommodate the wider bandwidth requirement. The input noise power will also vary as the square of the bit rate until B^3 dependence becomes dominant as it is in high-impedance design.

One of the most important receiver characteristics to be addressed is the dynamic range. In practical systems, the receiver has to operate not only at the minimum detectable power (the sensitivity of the receiver) but also at optical power levels which can be significantly larger. This wide range of received power levels is caused by variations in repeater spacing, connector and splice losses, fiber losses, transmitter output changes with temperature and aging of different devices. This requirement is very important for local area networks where some transmitters are so close to some receivers.

The receiver dynamic range can be defined as the difference (in decibels) between the minimum detectable power level and the maximum allowable input power level. As the received optical power increases the bit error rate decreases because of higher signal-to-noise ratio is obtained. This improvement continues until saturation or overloading occurs at the receiver (in this thesis preamp has an on chip automatic gain control loop to prevent overloading). At this point the received signal becomes distorted and the error rate starts to increase due to intersymbol interference.

The dynamic range is a function of the load resistor the feedback resistor of the front-end receiver preamplifier. As the feedback resistor decreases, the maximum allowable received optical power increases. However, as we know that decreasing the feedback resistor value will increase the noise level. Thus there is a tradeoff between high receiver sensitivity and wide dynamic range.

CHAPTER 4

LIMITATIONS OF PRIOR ART DESIGNS

With a practical system there are limitations on power supply voltages and transistor/device technology which place a finite limit on the amount of open loop voltage (A_V), and output voltage swing available. Even without practical limitations, an indefinite increase in open loop gain will result in increasing phase delay through the amplifier via the Miller effect. When combined with increasing loop gain (lower R_f) and increasing loop bandwidth, increased open loop gain will decrease phase margin when feedback is applied via R_f because large open loop gains are usually accompanied by large phase shifts (reduced phase margin due to Miller multiplication of input to output capacitance by A_V) which can make the TIA unstable, resulting in peaking frequency response and oscillations. Therefore once a high gain, high bandwidth and low phase shift open loop amplifier is designed, and given the fact that the input FET size and FET noise is set by the requirement that its C_{gs} match the photo detector, the most realistic design variable left for an optimized design is that of the feedback resistor.

Prior art TIA designs have required that high sensitivity be sacrificed for wide dynamic range and wide bandwidth since from equation (3) it can be seen that increasing R_f will decrease bandwidth and from equation (4) decreasing R_f will increase noise, and from $V_{out} = Iin * R_f$ there is a limit on the available output voltage swing for a given R_f without incurring large amounts of pulse width distortion (if the output voltage exceeds about 1 Volt peak to peak a typical GaAs amplifier will begin to clip and lose its virtual ground at the input/feedback node). Noting that R_f is the most practical element to vary, an optimum TIA design would include a mechanism to vary the value of R_f under different input signal conditions (i.e. varying amounts of average input current). For instance, lowering the value of R_f during high input current conditions would keep the output voltage swing to an acceptable value and reduce the amount of pulse width distortion at the output of the TIA (at higher input current levels the noise generated by the lower value feedback resistor would be inconsequential, since the input signal is well above the noise level). Prior art designs have used discrete components to achieve the 622Mb/s bitrate with high sensitivity or a FET (with its V_{gs} set by resistor trimming voltage divider) in parallel with the feedback resistor to adjust transimpedance gain to optimize the receiver for different bandwidths and bitrates. The latter configuration proves difficult to manufacture as the channel resistance of a FET is extremely temperature sensitive with the net result being an unpredictable receiver transfer function variation over temperature. Also there have existed TIAs with on chip AGC FETs that have required external control circuitry.

ANADIGICS, Inc. in Warren New Jersey was successful in designing and manufacturing a GaAs MESFET TIAs integrated circuit that included an internal AGC circuitry that did not require any external control circuitry (ATA06211) where they guarantee -31dBm optical sensitivity (parameter is guaranteed - not tested - by design and characterization data at 622Mb/s, assuming detector responsivity of 0.9), 0 dBm optical overload and a transimpedance of approximately 2.5 KΩ. The ATA06211 has been in production for the last 4 years. One of the latest papers written on a low noise 622Mb/s GaAs MESFET transimpedance amplifier [17] was claiming an average input-referred noise current of <

$2pA/\sqrt{Hz}$ over 500MHz bandwidth and a self-contained AGC which extends dynamic range without external components. No further information was obtained since the paper was fairly new at the time of this thesis.

As we know that in optical receiver after a preamp a postamp is required for extra gain and due to economical reasons a much higher sensitivity is recommended since for each 1dBm increase in sensitivity the repeater spacing can be increased by approximately 5km. The circuit of this thesis was designed to have a higher gain with a three stage topology and a better sensitivity compared to past designs.

CHAPTER 5

AN AUTOMATIC TRANSIMPEDANCE CONTROL AMPLIFIER (ATCA)

5.1 Design Overview

This design has an on-chip transimpedance control circuit that provides extremely high input overload current capability and absolute phase margin stability during large input current conditions. Shown in Figure 7 is the circuit diagram of the (ATCA) and in Figure 8, that of a block diagram summarizing the functionality of the design. All FETs are depletion mode MESFETs and require a negative gate to source voltage for proper biasing. Q1-Q2 make up the first gain stage which is level shifted through two diodes (D1,D2). Diodes D5 and D6 level shift the source of Q1 so a single positive power supply can be used (Vdd). The differential second stage consists of Q4-Q8 and is fed via the level shifted output of Q2 connected to Q5 and via the connection of Q6 to the input of the ATCA (a third stage similar to Q4-Q8 is added to add more gain, and hence). This connection of the input signal to the gate of Q6 generates a zero in the transfer function at $1/R_f C_{gd\,6a}$, which enhances the stability of the amplifier [1],[6]. Q10 and Q11 function as a source follower (Q10) buffer to isolate the high impedance drain output of Q6a and to provide a one diode voltage drop (D7) so the V_{gs} voltage at Magc1 , Magc2 and Magc3 will be negative under low input current conditions. When the Vgs voltage on Magc1, Magc2 and Magc3 is negative both FETs will be turned off, allowing the ATCA to effectively operate as a fixed feedback resistance TIA. Q13 and Q12 form another

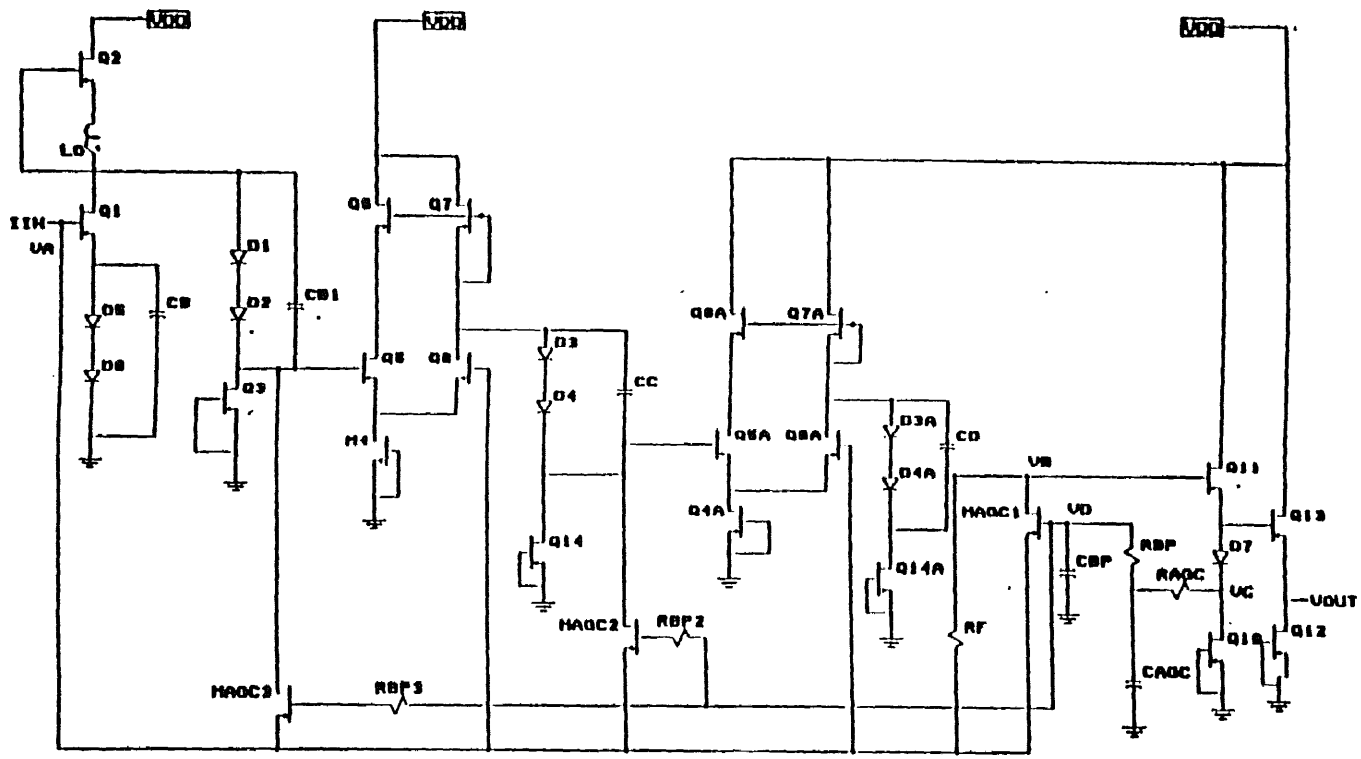

Figure 7 Automatic Transimpedance Control Amplifier

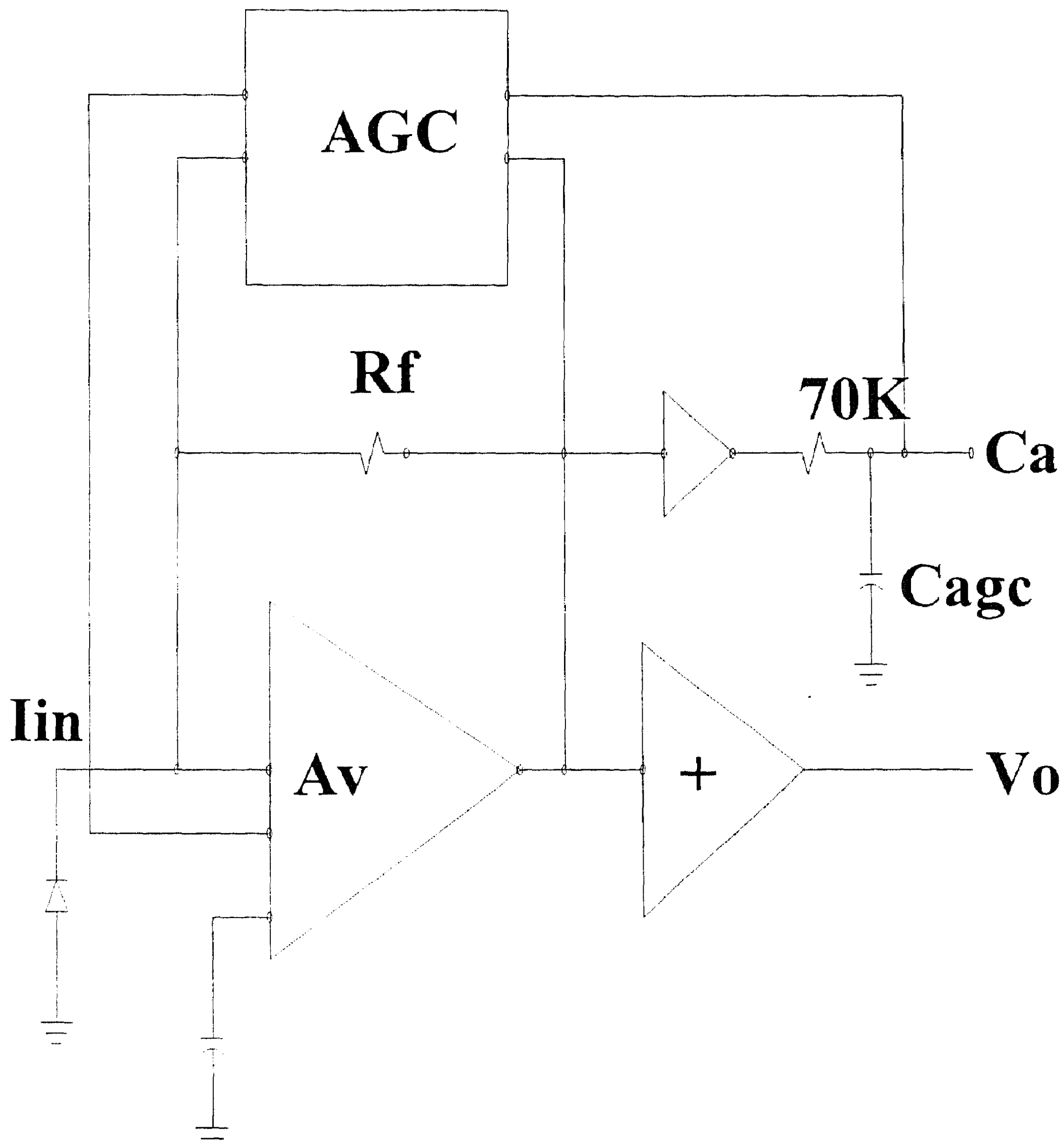

Figure 8 ATCA Functional Block Diagram

follower buffer to drive external low impedance (50 ohms) transmission lines. The FET MAGC1 is connected in parallel with R_f and its gate is fed the average value of the level shifted unbufferd output voltage via RAGC, CAGC (forming a single pole low pass filter), and via Rbp and Cbp (forming a single pole bootstrapping circuit which will be explained later). The gate of MAGC2 is connected to the gate of MAGC1 via RBP2 and functions to reduce the gain of the second stage by reducing the load impedance seen by the high output impedance of Q6 , the gate of MAGC3 is connected to the gate of MAGC1 and MAGC2 via RBP3 and helps to reduce the gain of the first stage by reducing the load impedance seen by the high output impedance of Q1. As the average optical input level increases, a negative current flows out of the input and the gate of MAGC1 (node V_d) MAGC2, and MAGC3 is turned on with a positive gate Vgs voltage. The AGC circuit operation will be discussed in details in Chapter 6.

5.2 Hardware/Test Procedure

The specific purpose of this section is to outline the procedure used to simulate and measure this three stage transimpedance amplifier described in this thesis. A wide variety of test equipment was used to guarantee the results of every and each measurement. Starting with the simulation tools, SPICE was used for all the simulations (results will be shown in Section 5.3) the FET models for a depletion mode MESFET were provided by ANADIGICS, Inc. in Warren New Jersey, with all the equipment required for measurements as described below:

- Controlled software using Microsoft© Visual Basic™ written by Tim Laverick, manager of fiber optics ICs in ANADIGICS, Inc.

- Scalar Measurement System, Wiltron 5417A
- Power supply, HP6624A
- Multimeter (Qty. 4), HP3478A
- Power meter, HP438A
- Power sensor, HP8484A
- Communications Signal Analyzer CSA803, Tektronix
- ANRITSU Signal Pattern Generator

A block diagram for the test station is shown in Figure 9

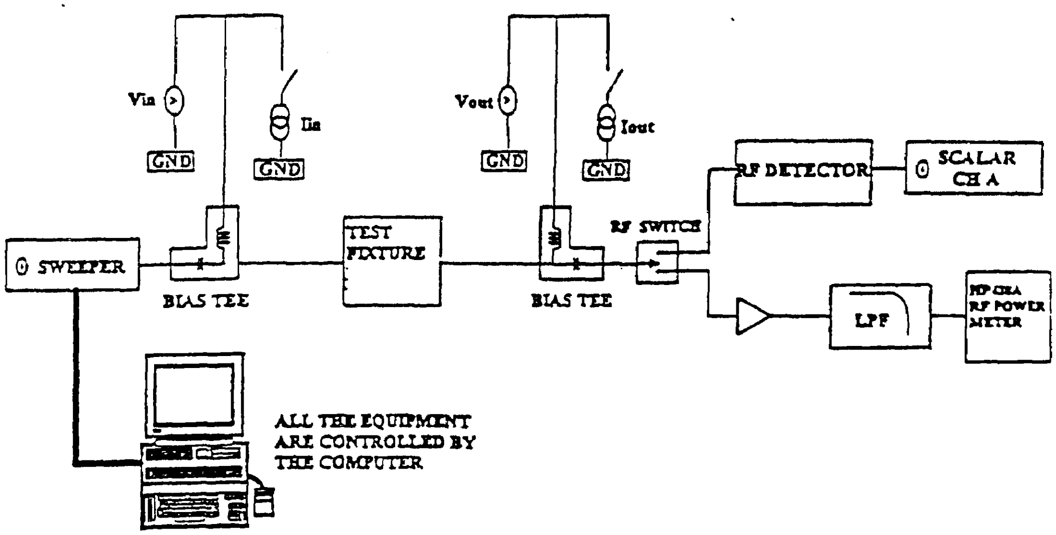

Figure 9 Test Station Block Diagram

5.3 Measurements and Results

One of the first simulation was done to guarantee no peaking or oscillations were occurring from the increase of the open loop gain since I was using a three stage topology to improve the gain of this transimpedance amplifier. As shown in Figure 10 the simulation for the TIA has a transimpedance of 77 dB (Log scale was used on x axis) and a bandwidth of approximately 680 MHz over three different bias (5.5, 5.0 and 4.5 Volts) with slight change in bandwidth and gain. Using lower voltages (below 4.5 Volts) will degrade the bandwidth, overload and sensitivity since this circuit was designed to operate on a single supply, therefore, lowering the voltage will push the FETs to operate in the linear region and thus, will provide insufficient gain. These results were obtained by using in the simulations a photodetector capacitance of approximately 0.6pF since we know from equation (3) that an increase in capacitance a decrease in bandwidth will result, and since most of the popular PIN detectors available in the market today have a value of approximately 0.6 pF. On the other hand the measurement was done using a 10 lead flat pack as shown in Figure 11, where I included a chip in front of the TIA that has an equivalent photo diode series resistance of 5 kΩ, a 0.6 pF photodetector capacitance, and a 50 Ω a resistor and 220 pF capacitor in series for matching the 50 Ω of the scalar analyzer, this can be seen in details in Figure 12. Figure 13 will give us the results of the measurements done at room temperature (over three different voltages, 5.5, 5.0, and 4.5 Volts.) where we can see that the bandwidth was close enough to the simulation results, and a transimpedance of approximately 78 dB. The dip at approximately 150 MHz is due to bonding inductance's.

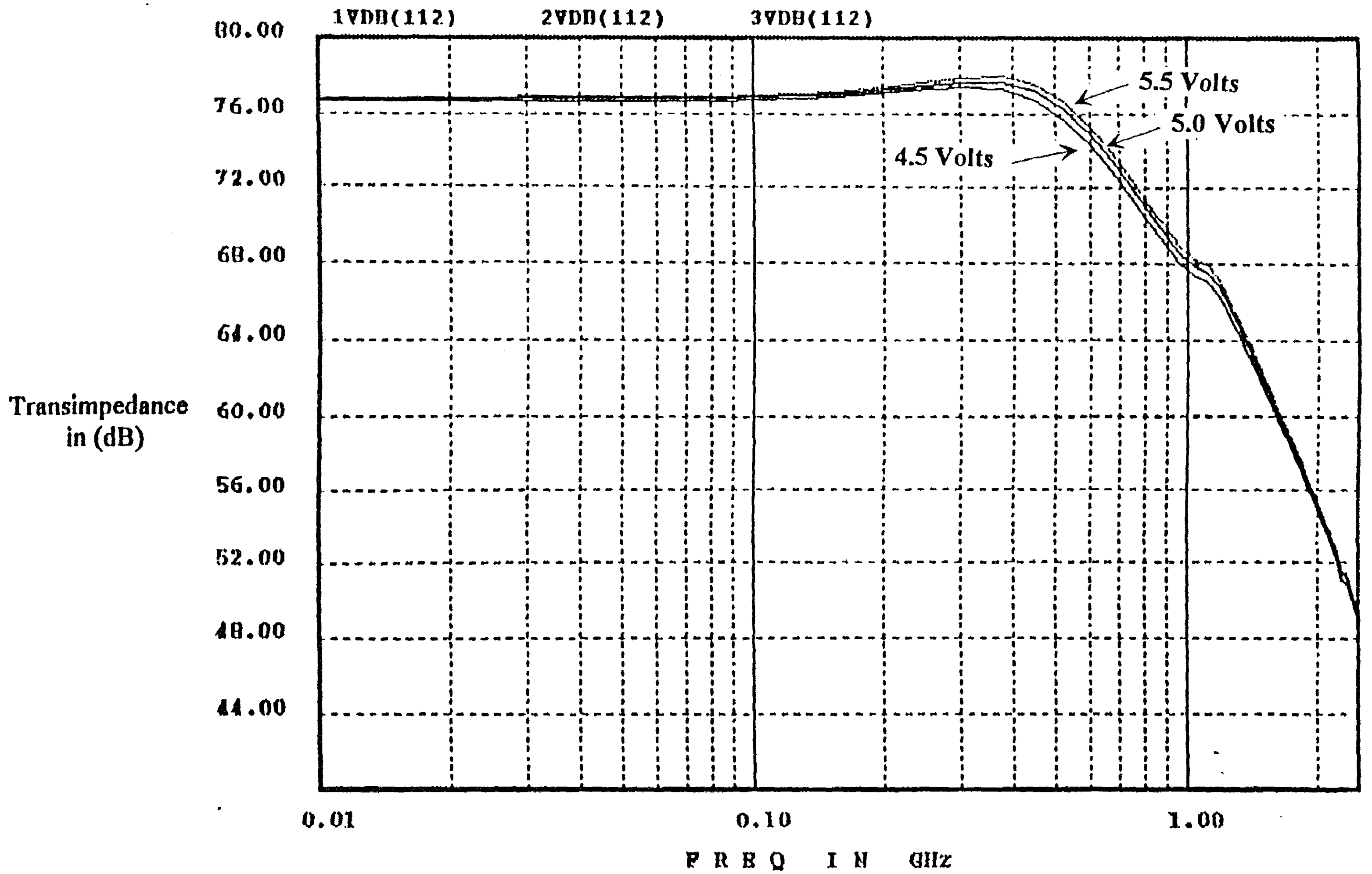

Figure 10 Transimpedance vs. Frequency (Simulations)

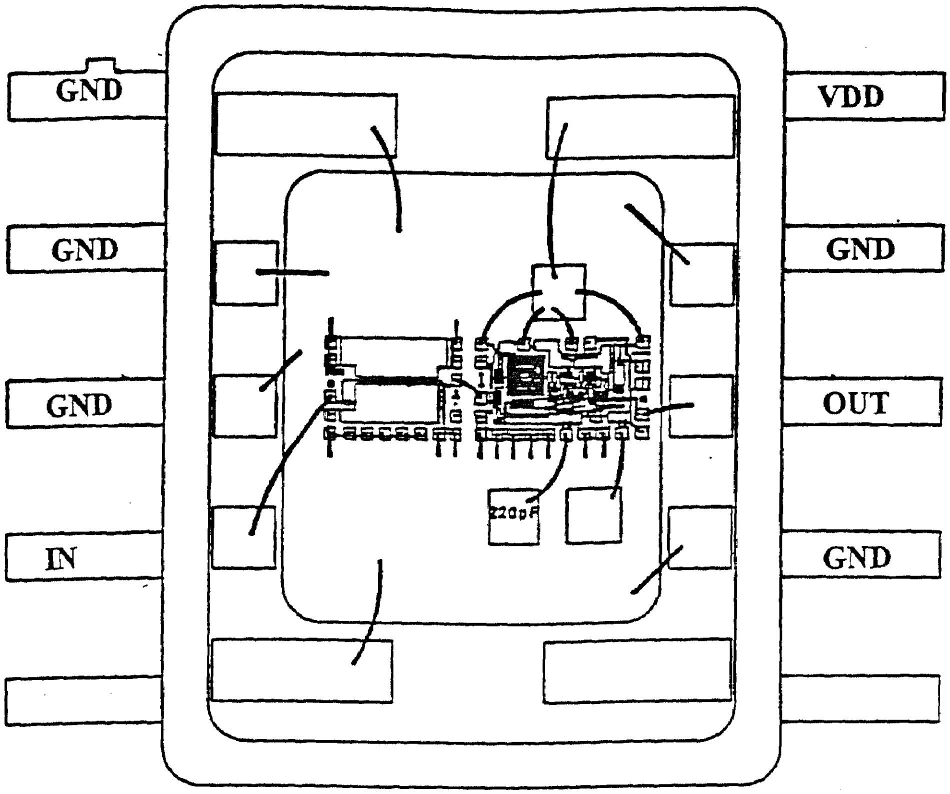

Figure 11 Package Bonding

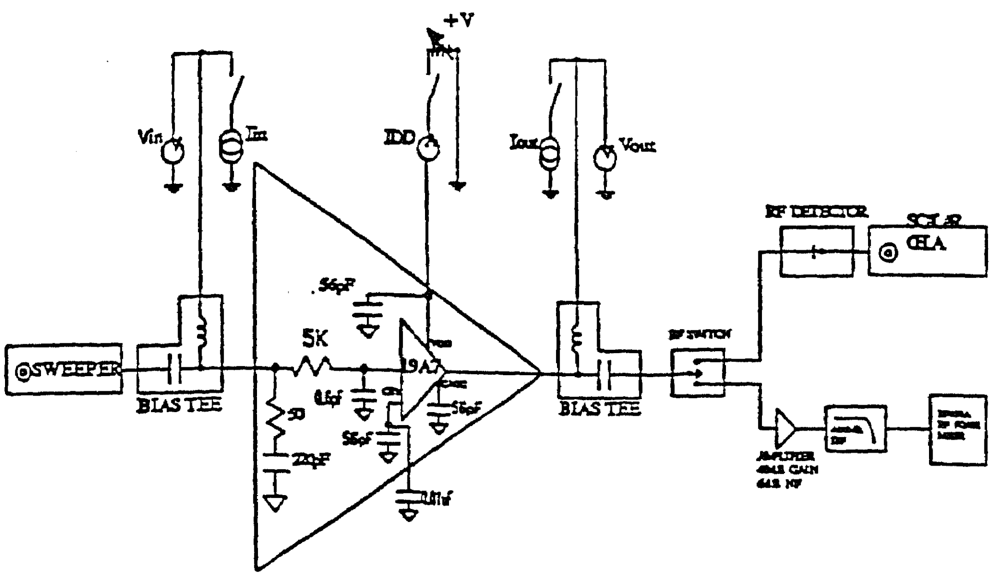

Figure 12 Detailed Test Diagram

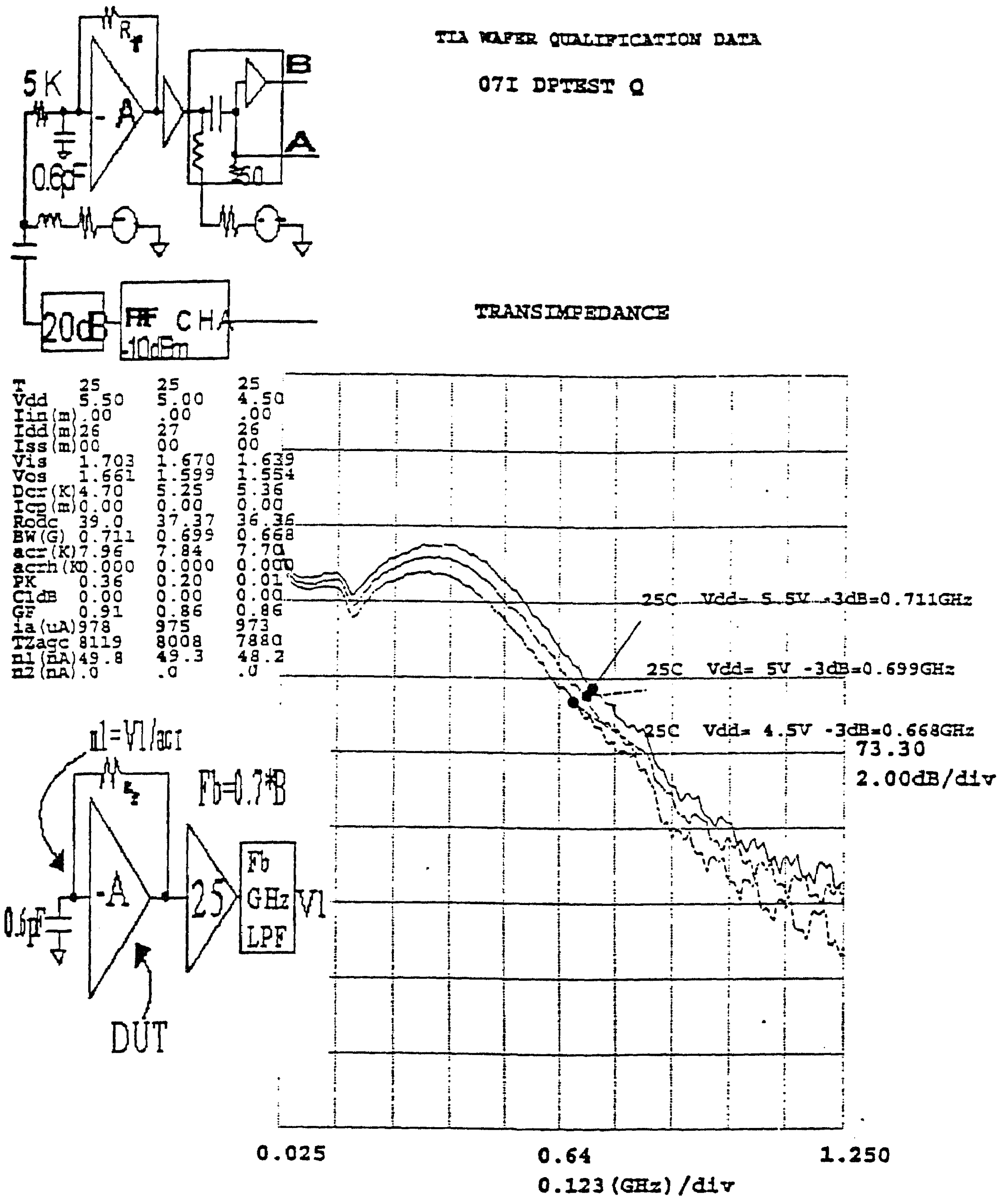

Figure 13 TIA vs. Frequency (Measurements)

Optical overload can be defined as the maximum optical power above which the BER (bit error rate) increases beyond 1 error in 10^{10} bits. An easy and accurate way to measure the optical overload is with a DC measurement which has an excellent correlation with an PRBS optical overload measurement. The measurement consists of sinking a negative current from the transimpedance amplifier and determining the point of output voltage collapse. Figure 14 shows the simulation results of the DC operation of the ATCA with the AGC circuit, from this curve one can see that with the AGC FETs connected, the output voltage does not collapse at currents up to 2600μA, because the output voltage swing is kept below 1 Volt peak to peak. Also the input node virtual ground during "heavy AGC" should be checked to verify that the linearity (i.e. pulse width distortion) of the amplifier has not been compromised.

The measurement consists of the following steps:

- Input offset voltage (Vis) is measured with Iin set to 0 mA.
- Vis and the output offset voltage (Vos) are measured with Iin(DC) set to -600μA (equal to -300μA average, -4.8dBm optical, assuming PIN responsivity of 0.9).
- Vos is measured with Iin set to -500μA.
- Delta Vis (Iin=0 to Iin -600μA) must be less than 30 mV.
- Delta Vos (Iin=-500 to -600μA)/100 must be > 250 ohms and < 1200 ohms.

Step 4 treats the TIA as a single input opamp with virtual ground at the input. In other words if the input offset Vis collapses by more than 30 mV while Iin=-600μA, then the linearity (pulse width distortion) of the amplifier is compromised at the BER increases dramatically. Figure 15 shows the measurements done over the range of three different

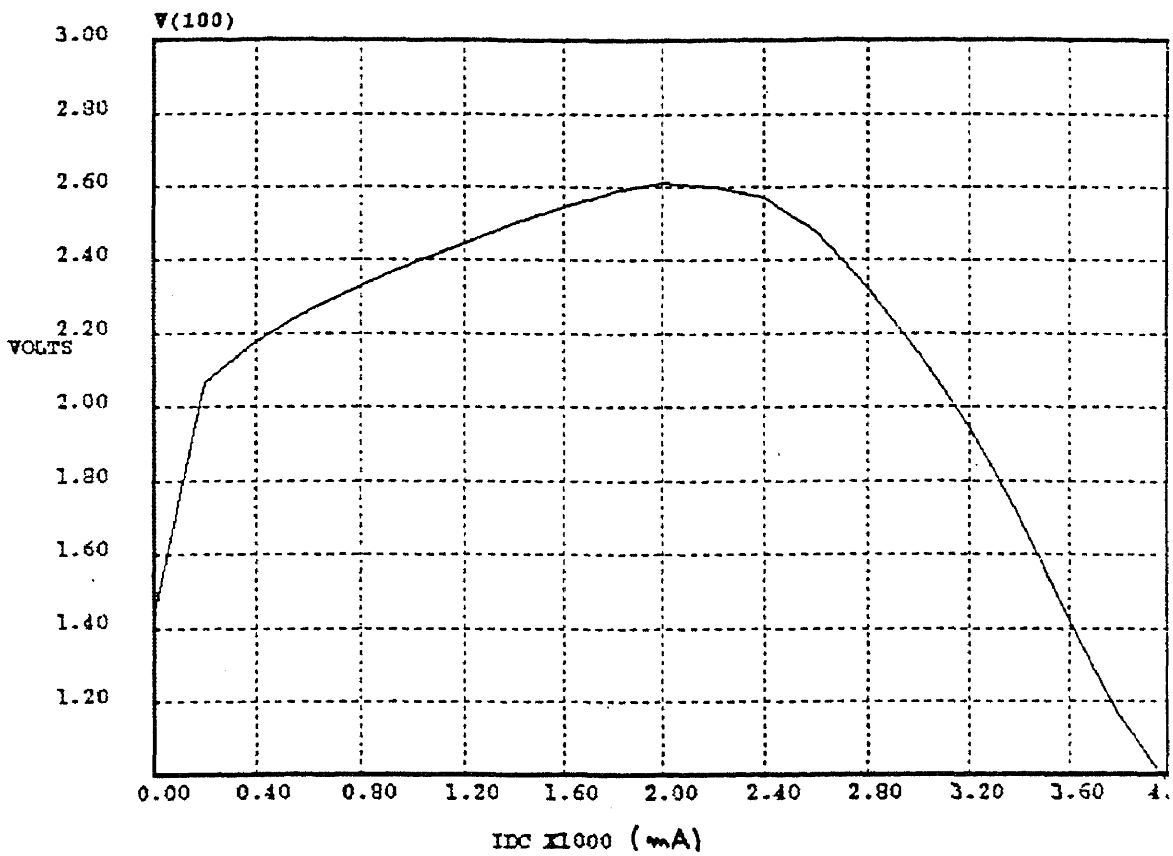

Figure 14 DC Transfer Curve (Simulations)

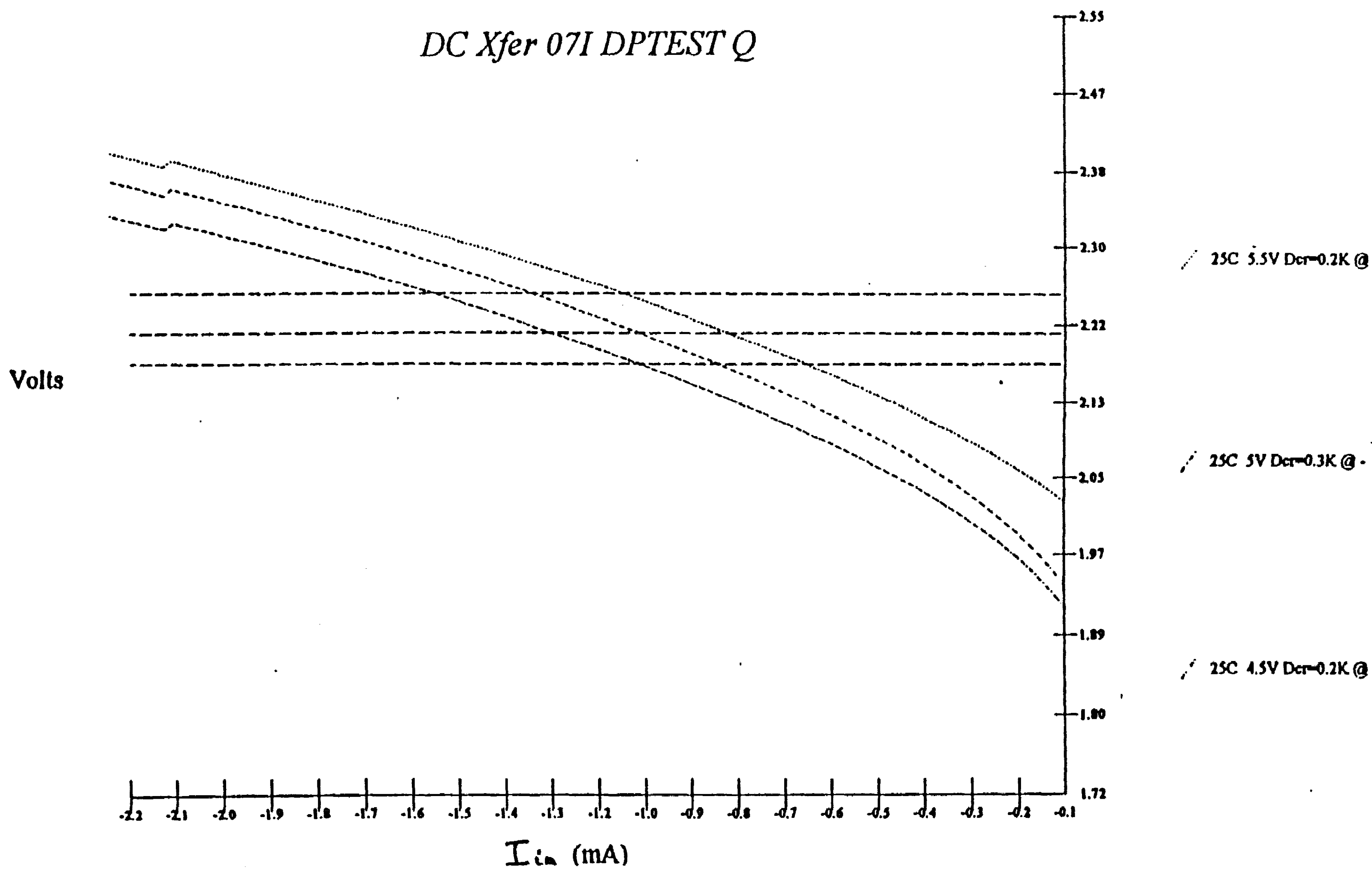

Figure 15 DC Transfer Curve (Measurements)

biasing (5.5, 5.0, and 4.5 Volts). It is important to select an external AGC capacitor of high quality and appropriate size. This TIA has an on chip 70KΩ resistor with a shunt 4pF capacitor to ground. Without external capacitance the chip will provide an AGC time constant of 280 ns. For the best performance in a typical 622Mb/s Synchronous Optical NETworks (SONET) receiver, a minimum AGC capacitor of 56pF is recommended (in the simulation and the measurement a 220 pF capacitor was used as shown in Figure 11). This will provide the minimum amount of protection against pattern sensitivity and pulse width distortion on repetitive data sequences during average optical power conditions. Conservative design practices should be followed when selecting an AGC capacitor, since unit to unit variability of the internal time constant and various data conditions can lead to data errors if the chosen value is too small.

The input referred noise spectral density was assessed in the simulation as shown in Figure 16 (over the range of the voltages mentioned before), where the input referred noise spectral density is in pA/√Hz versus the frequency. This value should be multiplied by the square root of the frequency range of interest as shown below,

i_n = (input referred noise spectral density pA/√Hz).(√low pass filter bandwidth Hz)

From equation (6) we can get the sensitivity of the device by assuming the responsivity of the photodetector 0.9 A/W. Knowing from [4] that the required bandwidth for the best noise performance in a SONET system is approximately equal to:

$$BW = 0.68 * \text{Bitrate}$$

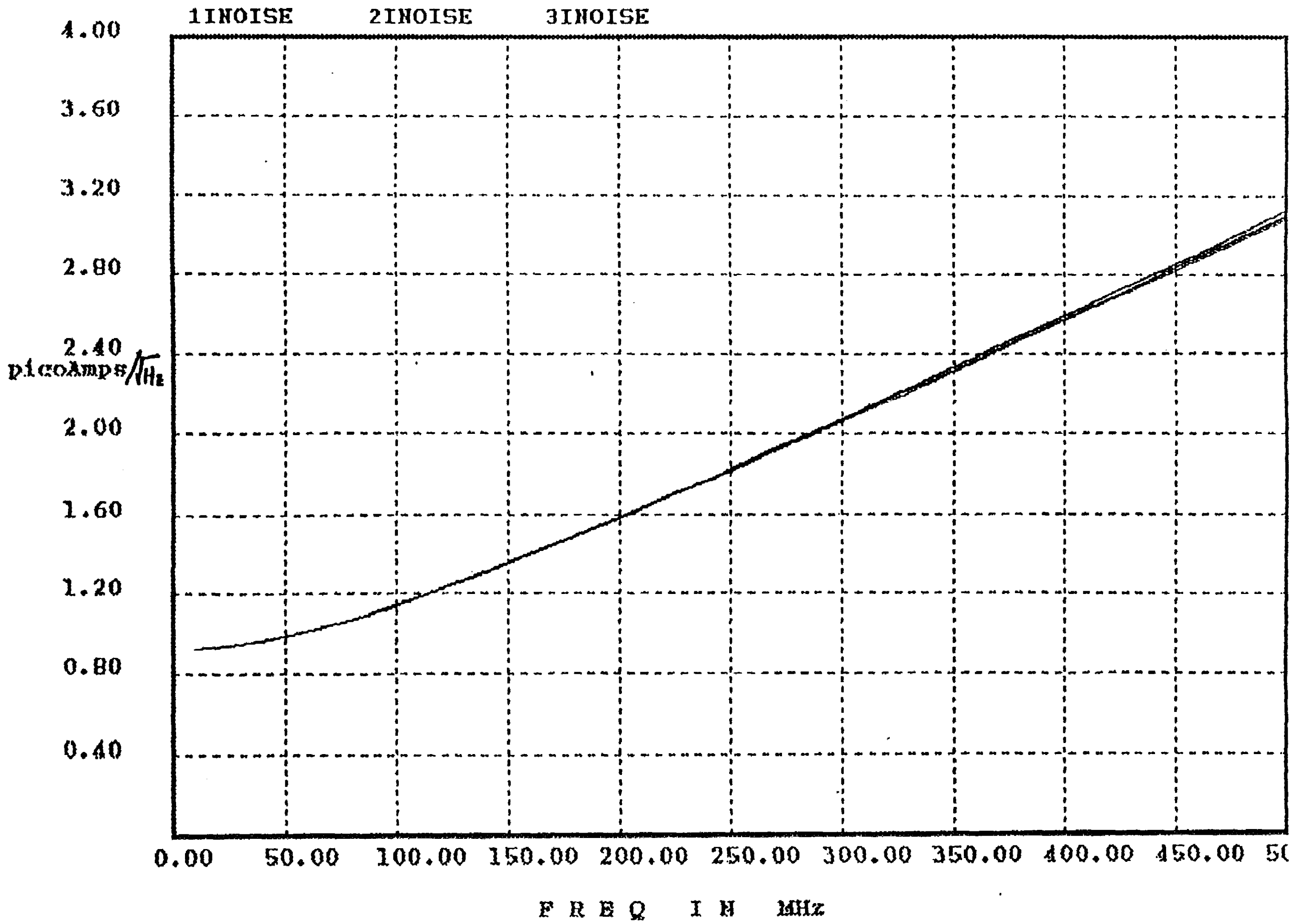

Figure 16 Input Referred Noise Spectral Density (Simulations)

a 400 MHz low pass filter was used. The purpose of the filter is to eliminate any extra noise owing from the extra bandwidth as shown in Figure 10 and 13. Therefore, multiplying the input referred noise spectral density in pA/√Hz by the square root of the 400 MHz low pass filter will give us ~ 49.5 nA. The noise measurement done on this device which is n1 (refer to Figure 13 for measured data over three voltages), an integrated noise current referred back to the input of the TIA as shown below in Figure 17. Using i_n ~ 50na and plug it in equation (6) will give us a sensitivity ~ -34.4 dBm. This test included a low noise amplifier (LNA) of 25 dB gain and a 400 MHz low pass filter and the RF power meter.

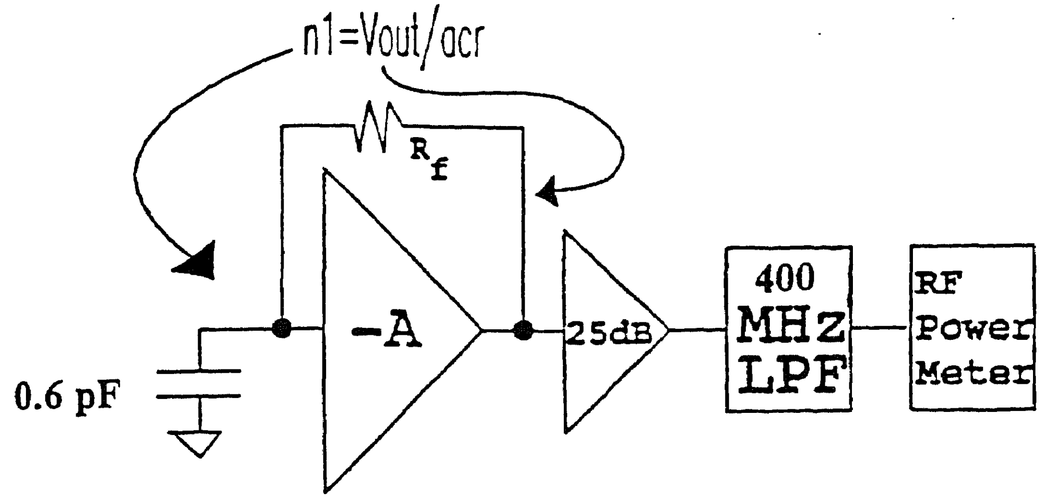

Figure 17 Input Referred Noise Current Test Diagram

As we can see the simulated data was close to the measured data within 2 to 3 % error margin. On the other hand the measured results may include extra inductance's and capacitance's due to bond wires, packaging, test fixture, and the fluctuation of the equipment used for the measurement. And these differences can be seen from one device to another due to the change in the parameters of the FETs that can be caused from the change in the process of the wafers.

Another measurement was done (yet not simulated) due to the limitations of the software used to simulate. This measurement consists of using a Pulse Pattern Generator which produces 2^{15}-1 Pseudo-Random Bit Signal (PRBS) in an NRZ form, which is known by the eye diagram test. The purpose of this test is to guarantee the opening of the eye and the 50% crossing which is the SONET requirement defined by Bellcore [21]. This measurement was done over three different temperatures(0,25 and 85 ° C) and three different voltages (4.5,5.0 and 5.5 Volts) as seen in Figures A.1-A.9. As we can see again the difference in voltages causes a slight degradation in gain due to reasons discussed previously. As one can see a slight overshoot is caused at higher voltages due to the extra peaking. Nevertheless these degradation either due to voltages or temperatures did not effect the BER test which was fixed at probability error of less than 10^{-10}.

A reliability test was done on this device, where a TIA was bonded as in Figure 11 and was powered up for approximately 30 days. The same device was retested and no degradation were found as seen in Figure A.10.

CHAPTER 6

AGC CIRCUIT OPERATION

It is important that current be drawn out of the input since this causes the source of the MAGC1 to be connected to the input and hence preventing pulse width distortion. The reason for this is that as the output voltage goes positive the input node (gate Q1) remains close to the zero input offset voltage (Vis, within a few tens of millivolts) since the input maintains a virtual ground. The V_{ds} on MAGC1 is then positive and the voltage at node V_d is positive with respect to V_a and Vgs_{MAGC1} is negative ($Vgs_{MAGC1} = V_d - V_a$), which effectively connects the source MAGC1 to the input node $V_{a.}$. The operation of the bootstrapping circuit (consisting of Rbp and Cbp connected to MAGC1) is the key to maintaining low pulse width distortion and wide bandwidth during large input current conditions. Figure 19 shows a small equivalent of AGC FET, MAGC1, including the C_{gd} and C_{gs} of MAGC1. Ragc and Cagc form a low pass filter to provide an average value of the output signal to the resistor Rbp. Rbp isolates or floats the gate of MAGC1 AC wise via the bootstrapping effect of C_{gd} and C_{gs}. This is important because it isolates the TIA from dynamic transimpedance variations (i.e. pulse width distortion). With limited rise time amplifiers as all real amplifiers are, an attempt to swing the output voltage above the saturated limits inherent to the design will result in clipping and pulse width distortion. Referring back to Figure 19, C_{bp} is the key element added to this design to bypass the input pole created by $C_{gs}*R_{bp}$ under high input current conditions, since the value of C_{gs}

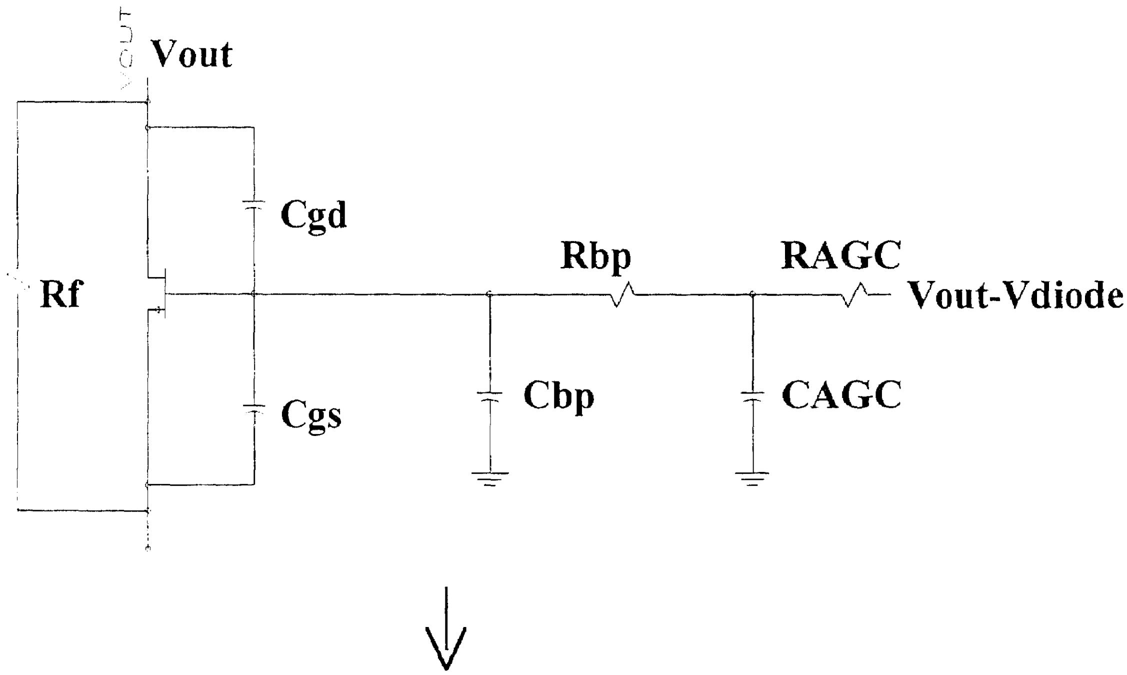

Small Signal AGC FET Circuit

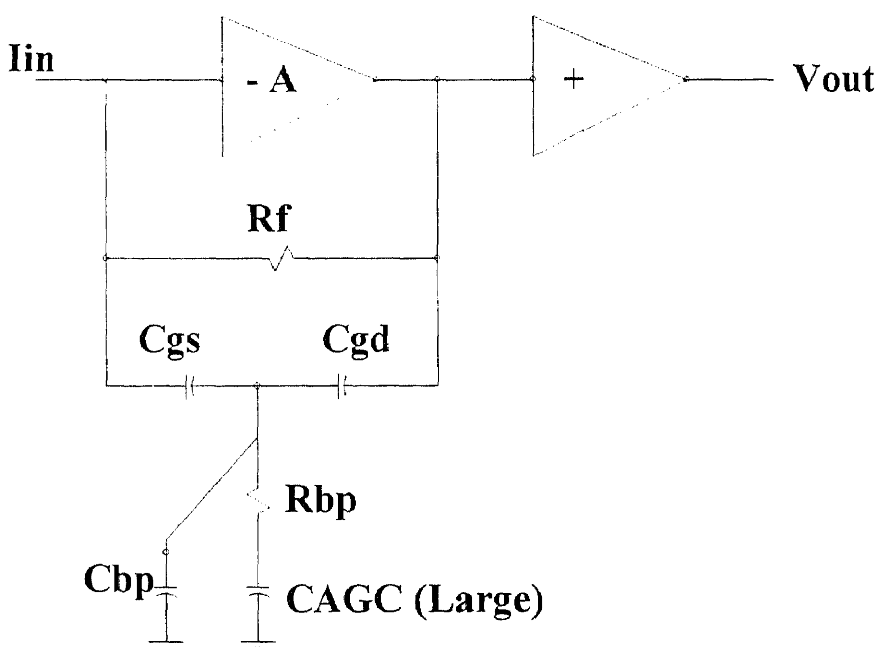

Figure 18 AGC FET

increases when the V_{gs} of MAGC1 increases. To prevent the TIA from oscillating when the value of feedback resistance is reduced via MAGC1 (and concurrently with increased feedback comes reduced phase margin) two things must occur: first the open loop amplifier phase delay must not increase, and second, the phase margin of the closed loop amplifier must not become negative. In the ATCA these criteria are met by decreasing the gain of the first gain stage (Q1-Q2) and the second gain stage (Q4-Q8)and the third (Q4a-Q8a) simultaneously. MAGC3 decreases the gain of the first stage by loading (adding resistance) in parallel with the Rd of Q1 and effectively the GmRd product of Q1. The gain of the second stage is reduced by a similar action on the drain of Q6 and the same procedure for the third stage using MAGC2.

CHAPTER 7

DISCUSSION

In this thesis, we have considered the design of a preamp used in optical receivers. Primary requirements of the optical receiver for various applications were identified. Tradeoffs between different receiver parameters have also been considered in detail. In particular, the receiver design for high-speed and high-sensitivity optical systems has been emphasized.

As far as receiver amplifiers are concerned, high-impedance, FET front-end, receiver amplifiers offer the lowest noise level up to few hundreds megahertz. Thus, they should be used for applications where receiver sensitivity is critical.

Above few hundreds of megahertz, transimpedance amplifiers are very attractive due to its inherent simplicity, wide dynamic range, and smaller receiver sensitivity degradation (compared to a high-impedance design).

In this thesis, the three stage transimpedance amplifier proved to be a very good preamplifier in a 622 Mb/s receiver due to several reasons:

• Single + 5 Volts supply, which is very critical when a power dissipation is an issue for the receiver module. This preamp will dissipate approximately 135 mW (results taken from Figure 13)

• Excellent sensitivity, which is a dominate factor in deciding the performance of preamplifier in optical receivers systems. Again, this TIA has a very good sensitivity with a -34.4 dBm. This improvement will allow a longer distances between repeaters and therefore lower costs.

• An on chip Automatic Gain Control (AGC). This will improve the dynamic range of the optical receiver since this TIA has an approximately + 3 dBm of optical overload. Thus this preamp can be used for shorter distances where the signal is still strong enough to cause some distortion if an AGC was not included. In addition, an on-chip AGC reduces the size and cost of the entire optical receiver module.

• Large enough transimpedance gain ($\approx$ 7.8 Kohms) so that a post-amp might not be required for some receivers depending on the sensitivity of the clock recovery and data regenerator chip.

Table 3, will give us a quick reference of the TIA performance.

As we can see from Table 3, that the dynamic range of this preamp is approximately 37 dBm which is very wide and therefore very efficient for today's stringent requirement for optical receiver systems.

Table 3 TIA Performance

PARAMETER	TYPICAL	UNIT
Transimpedance	7.8	kΩ
Bandwidth (-3dB)	700	MHz
Output resistance	38	
Supply current	27	mA
Input offset voltage	1.6	Volts
Output offset voltage	1.6	Volts
Optical overload	+ 3	dBm
Input noise current	49	nA
Optical sensitivity	- 34	dBm
Operating voltage	4.5 - 5.5	Volts
Operating temperature	0 - 85	° C

CHAPTER 8

CONCLUSIONS

A three stage transimpedance amplifier for fiber-optic receivers has been fabricated with a topology that improved sensitivity, dynamic range, and bandwidth. The improved sensitivity is derived from the use of an inductor FET load combination that reduces noise from the input stage of the amplifier [3], and by increasing the size of the feedback resistor. The bandwidth was not affected by the increase of the feedback resistor since we used a three stage amplifier that yields a larger open-loop gain than the previous two stage amplifiers. The three stage amplifier design was also shown to be stable enough to allow the use of an internal Automatic Gain Control circuit that varies the value of the feedback resistance and load the three stages at higher optical input signals.

An engineering lot of six wafers was processed at ANADIGICS, Inc. which included the circuit mentioned in this thesis. A low yield ~ 11 % was observed which is normal for an engineering mask. A study is being conducted now to improve the yield.

This three stage transimpedance amplifier can be used for the 622 Mb/s optical receivers (e.g. SONET OC-12) with an improved sensitivity and gain at the same time. And with varying the value of the feedback resistor with the same topology this amplifier can be used in different SONET systems.

APPENDIX

EYE DIAGRAMS

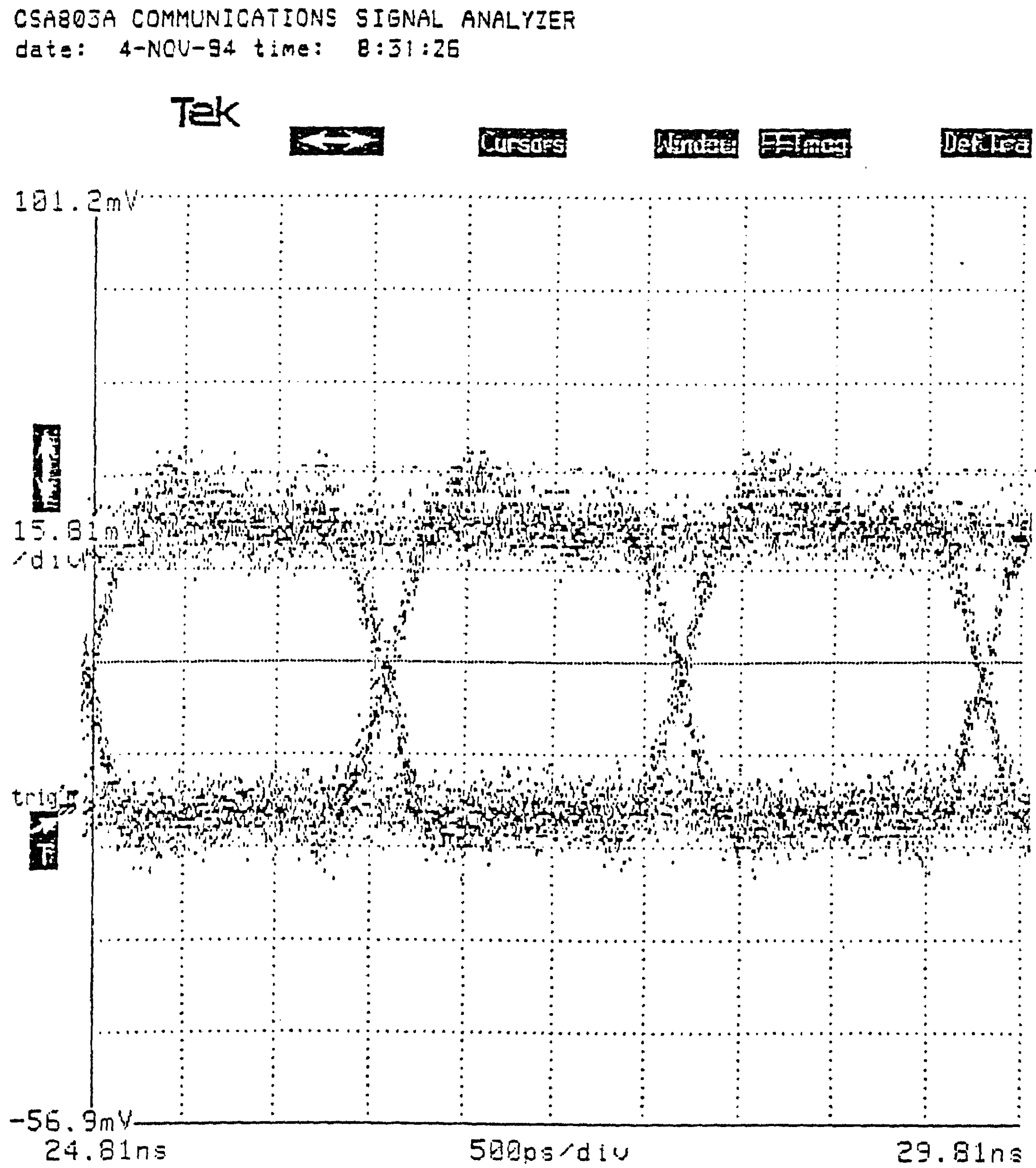

Figure A.1 Eye Diagram 0°C (5.5 Volts)

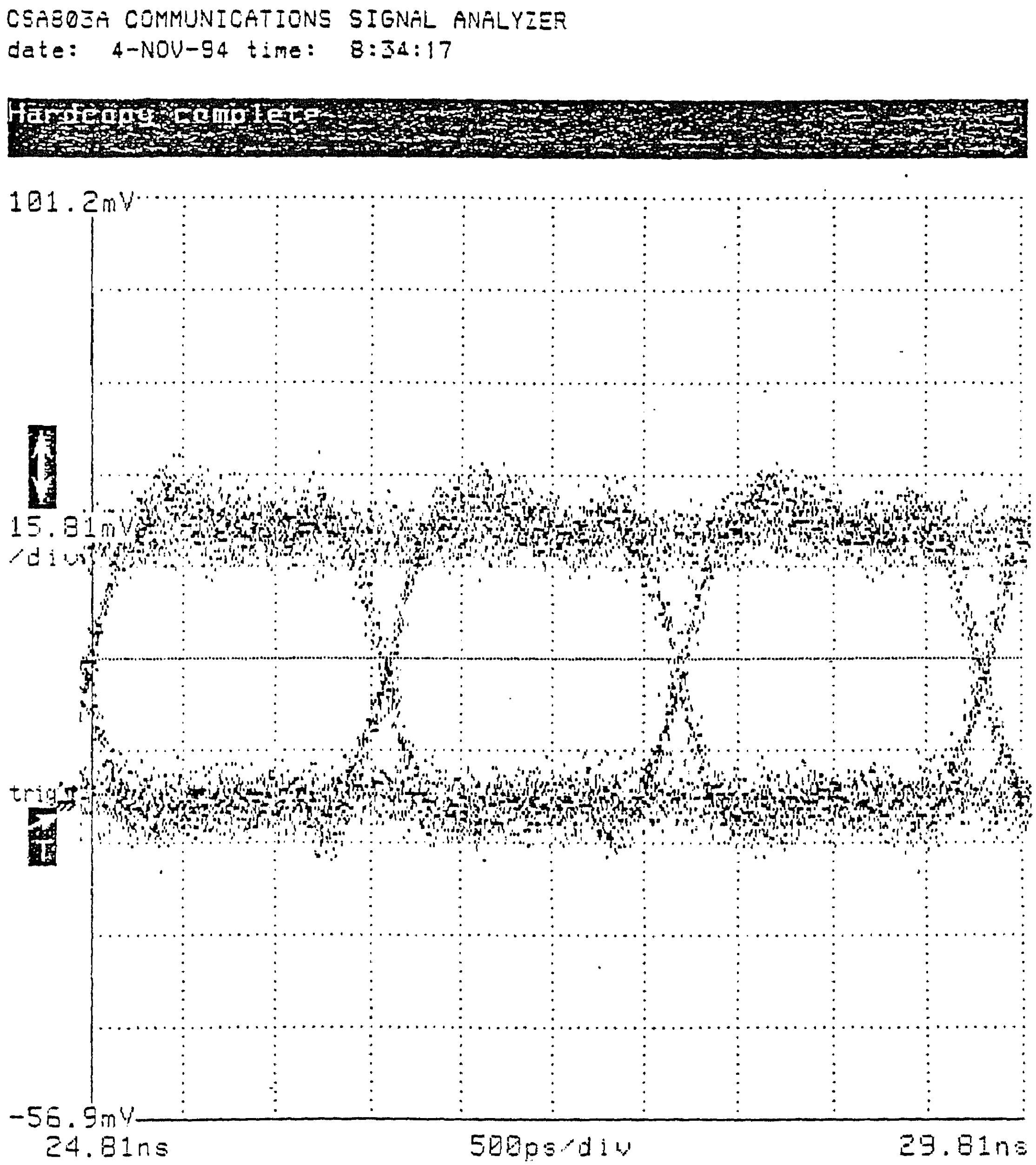

Figure A.2 Eye Diagram 0°C (5.0 Volts)

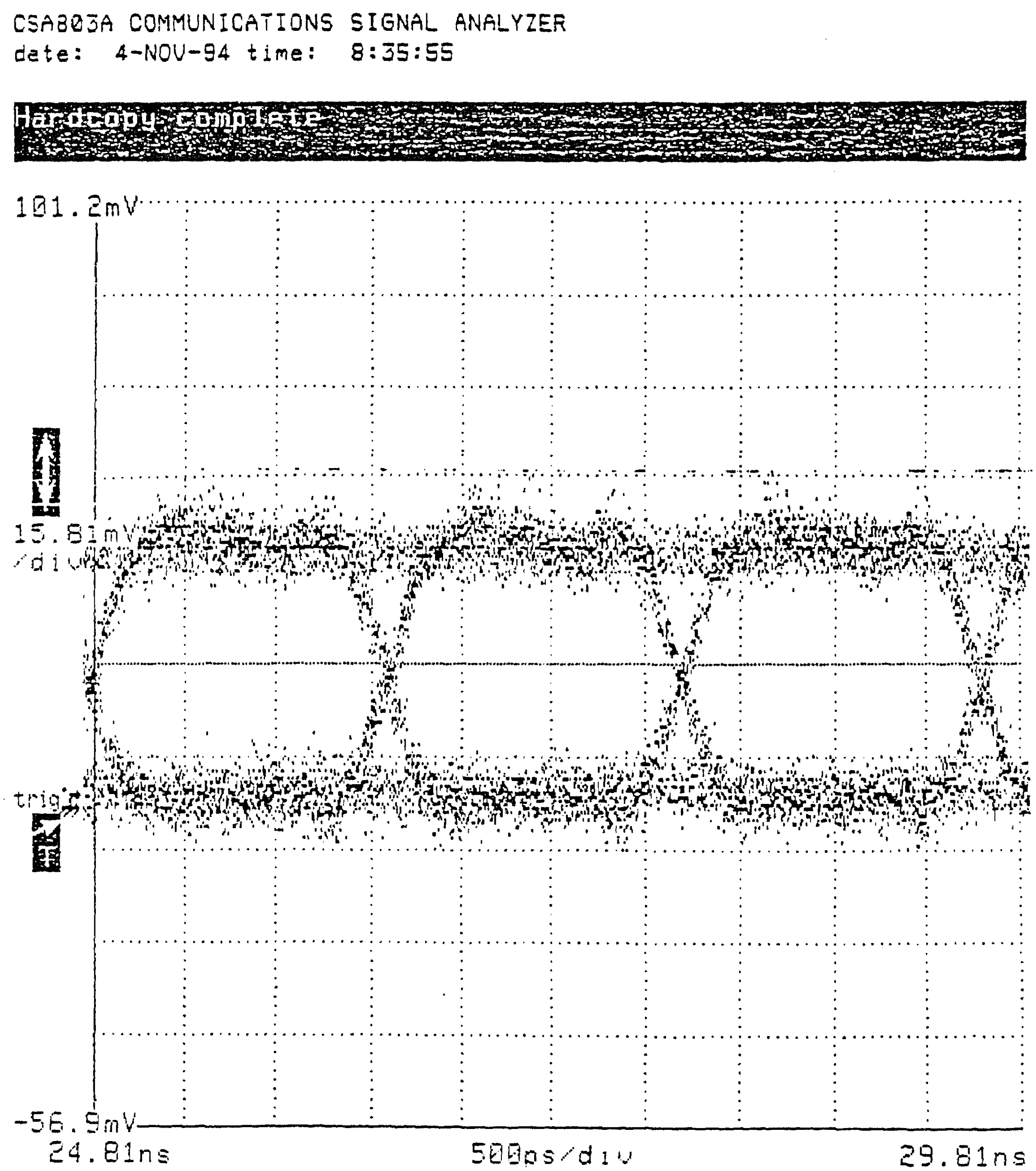

Figure A.3 Eye Diagram 0°C (4.5 Volts)

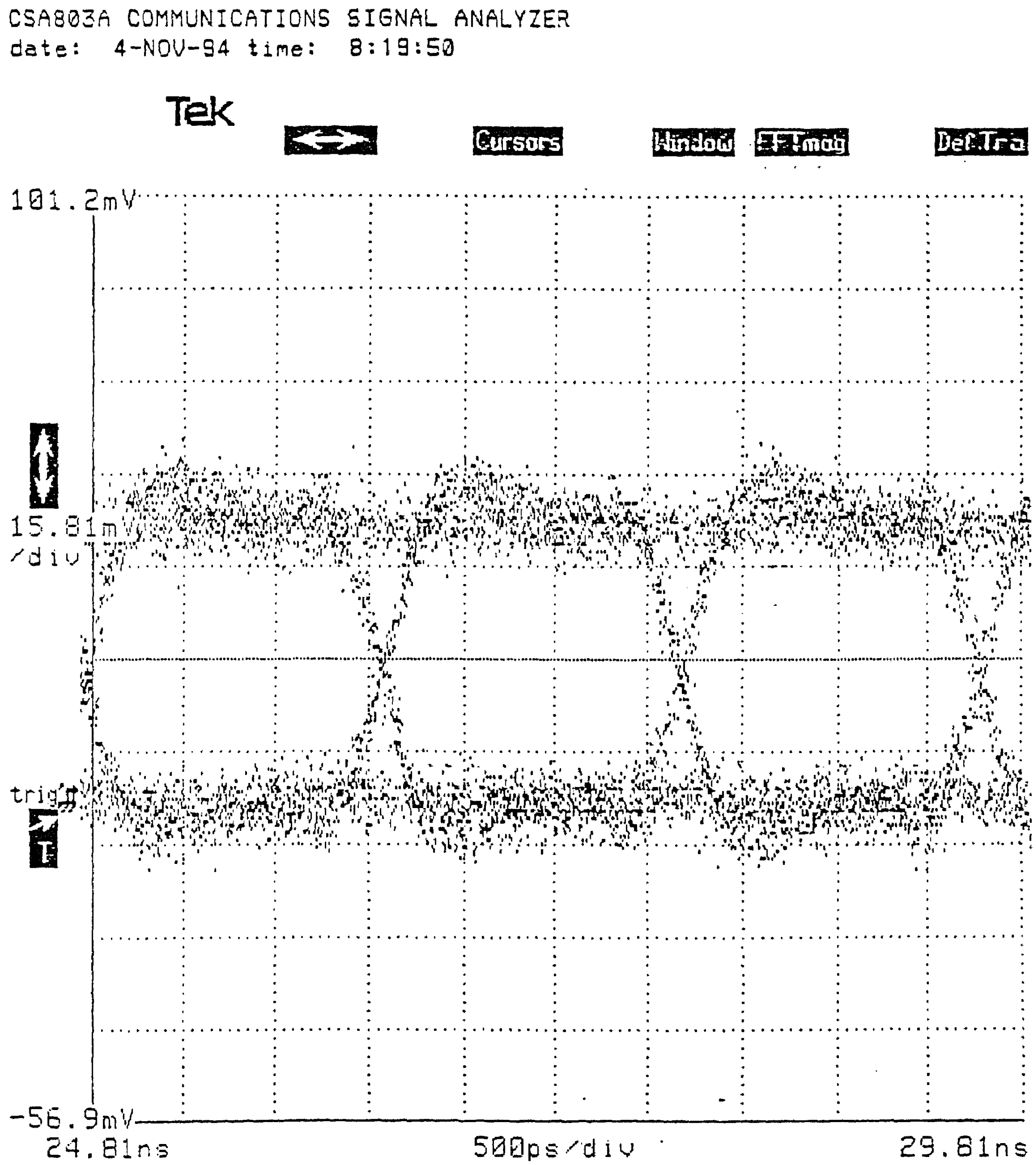

Figure A.4 Eye Diagram 25°C (5.5 Volts)

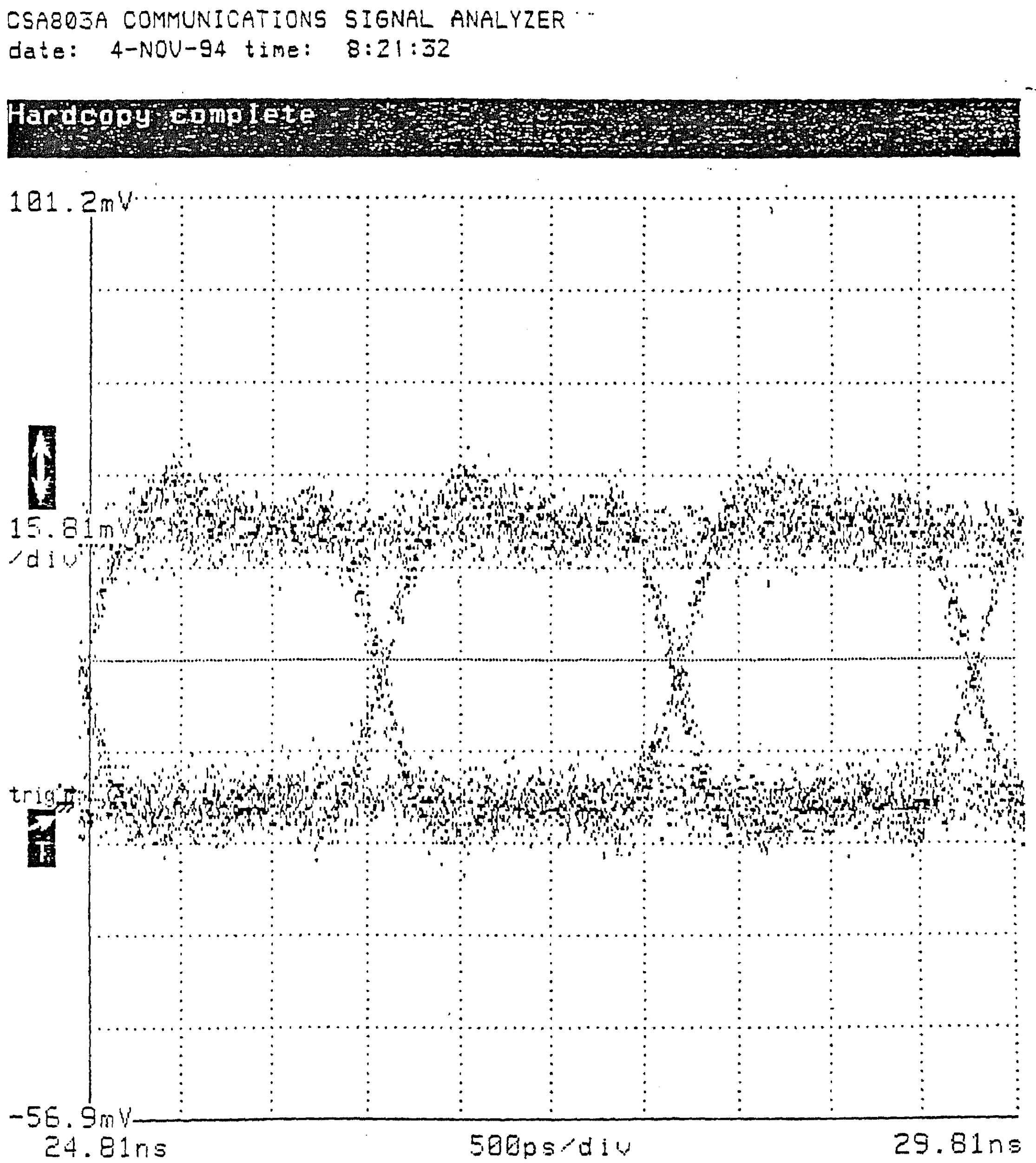

Figure A.5 Eye Diagram 25°C (5.0 Volts)

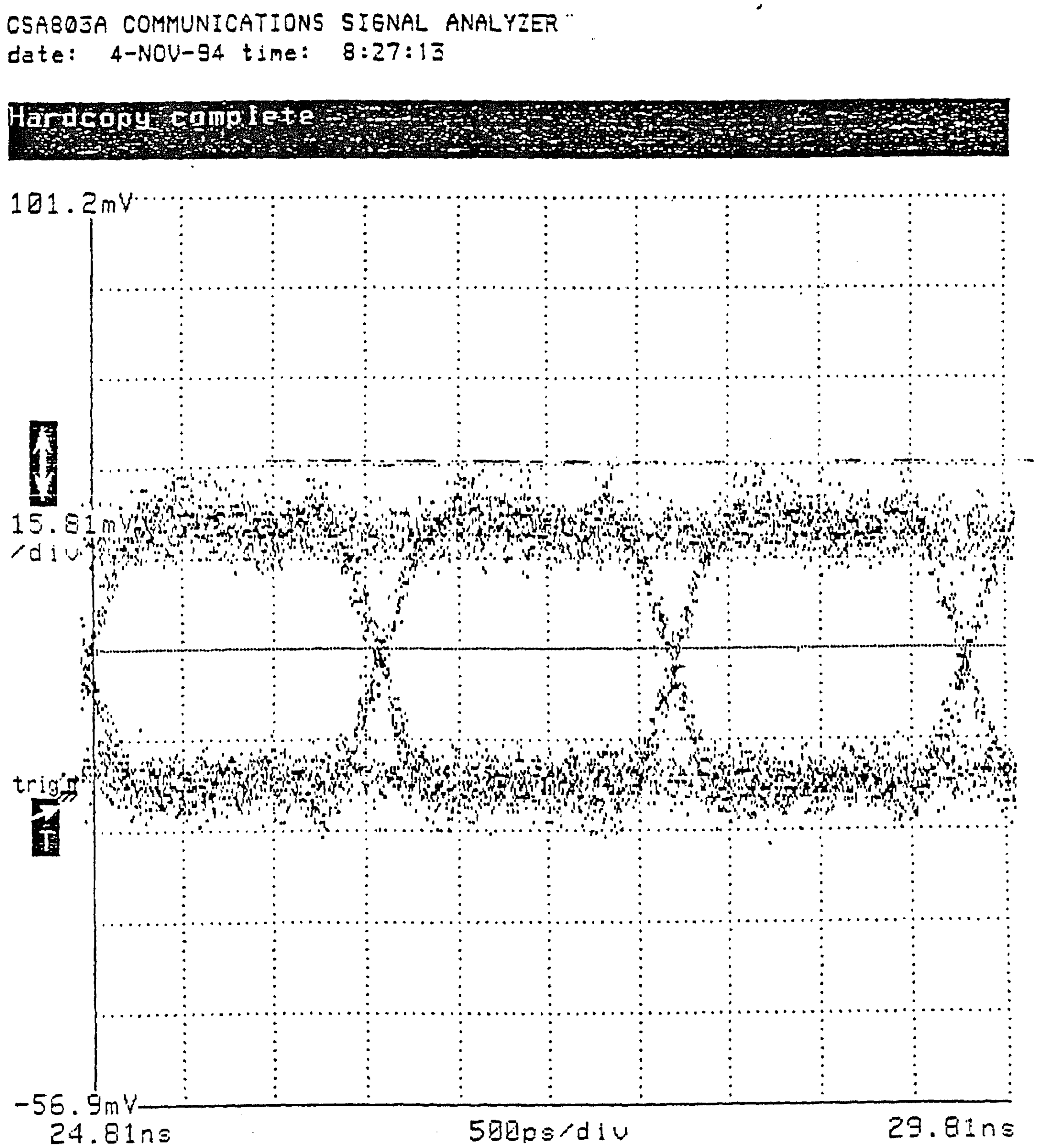

Figure A.6 Eye Diagram 25°C (4.5 Volts)

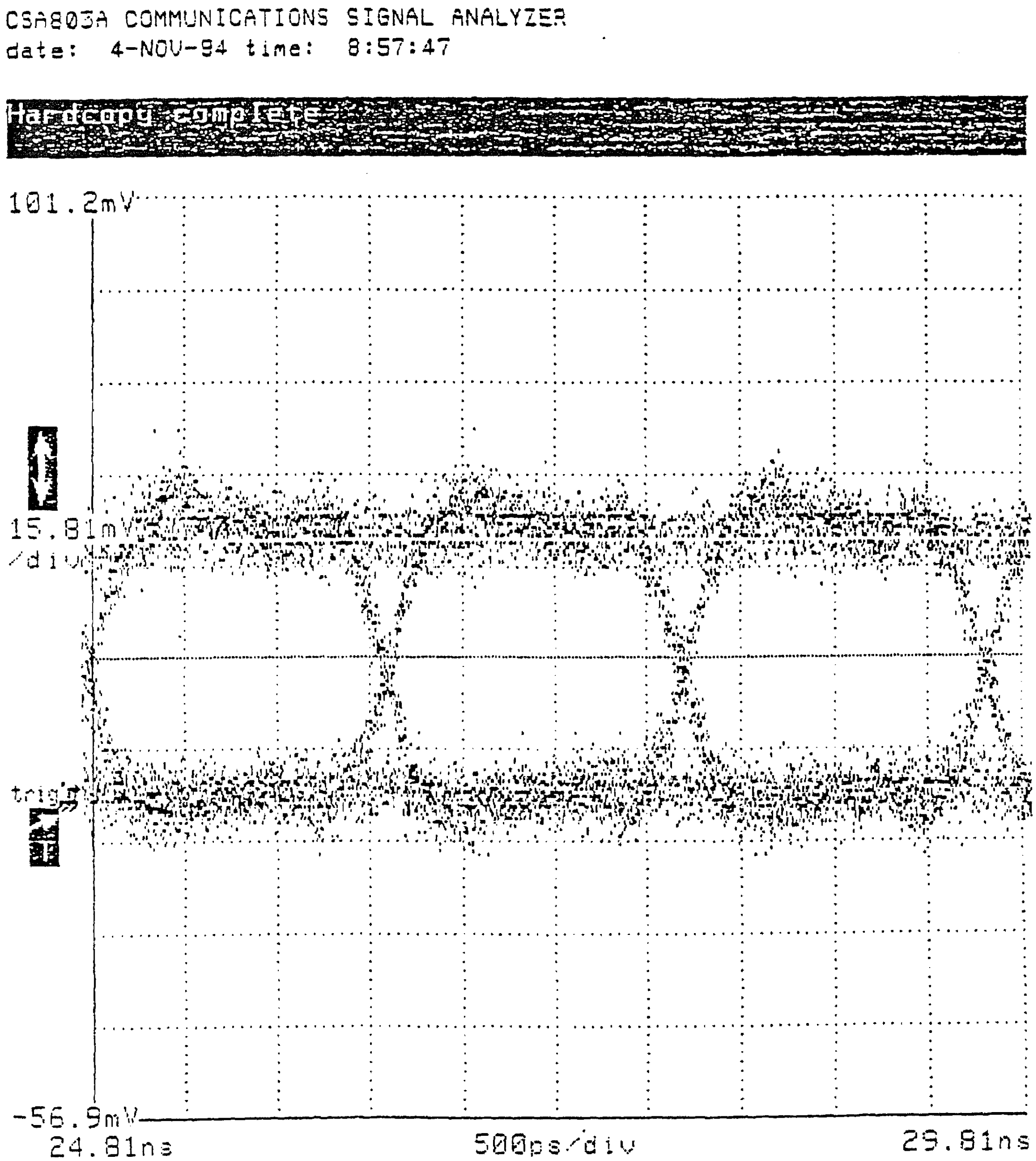

Figure A.7 Eye Diagram 85°C (5.5 Volts)

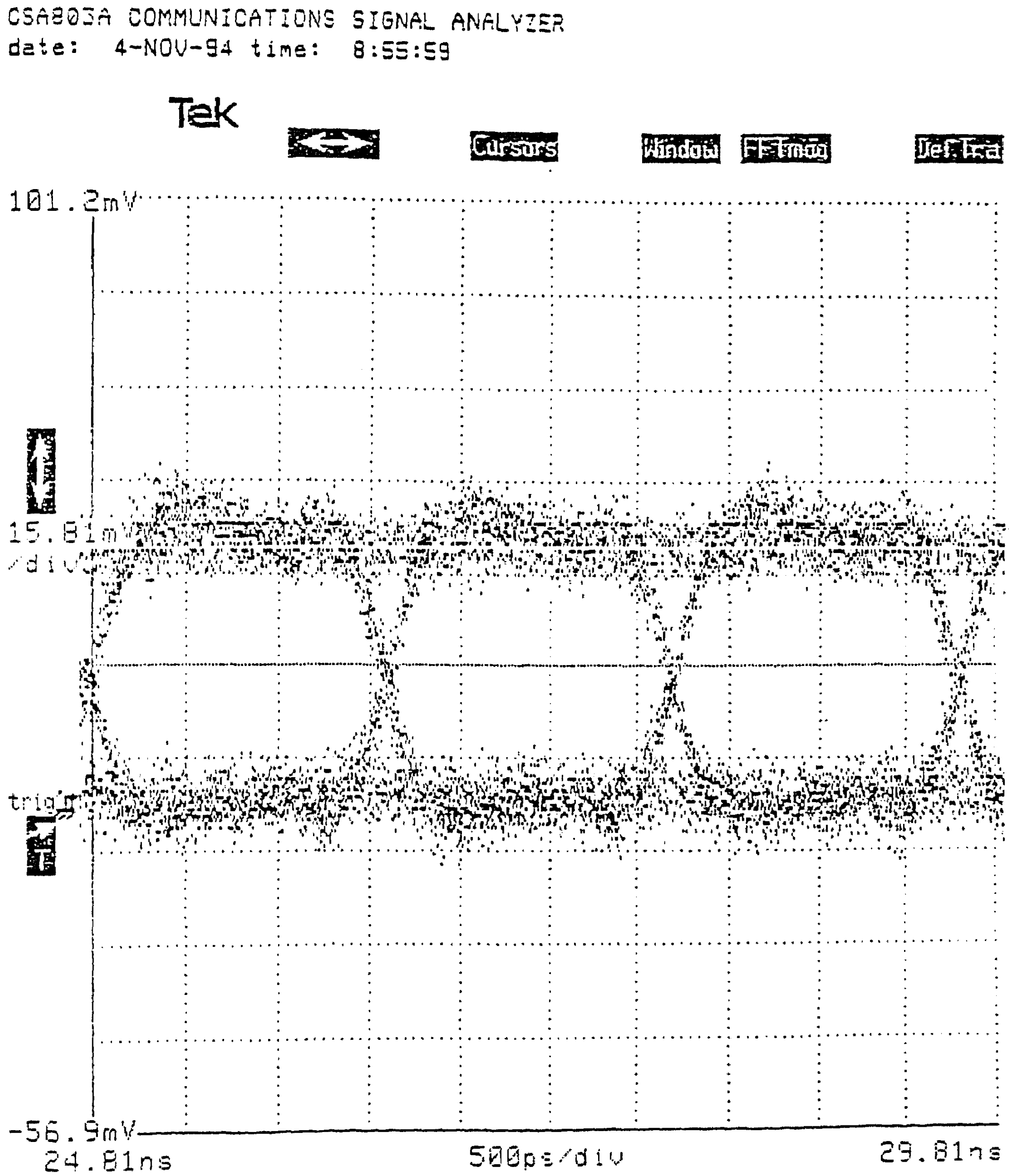

Figure A.8 Eye Diagram 85°C (5.0 Volts)

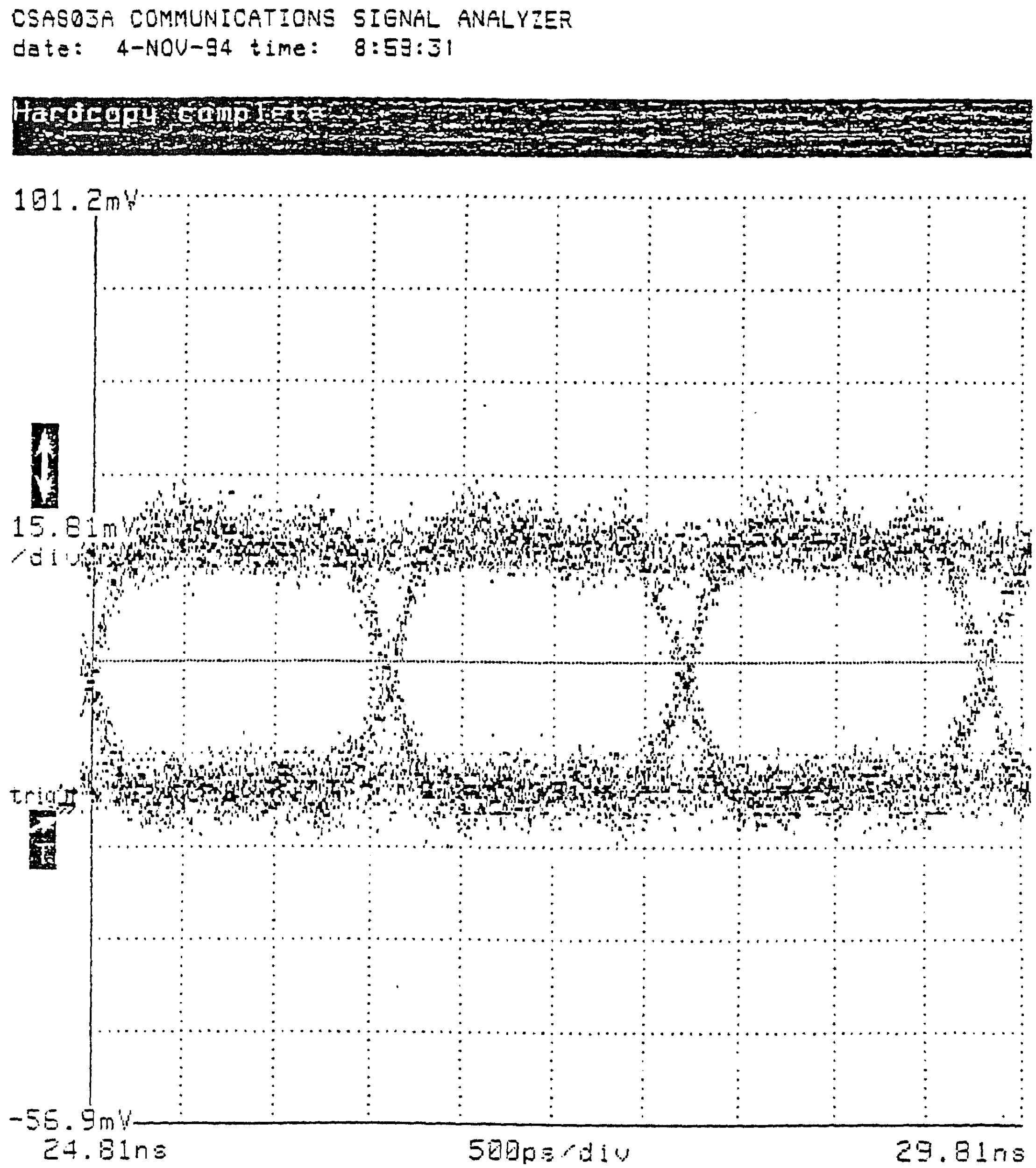

Figure A.9 Eye Diagram 85°C (4.5 Volts)

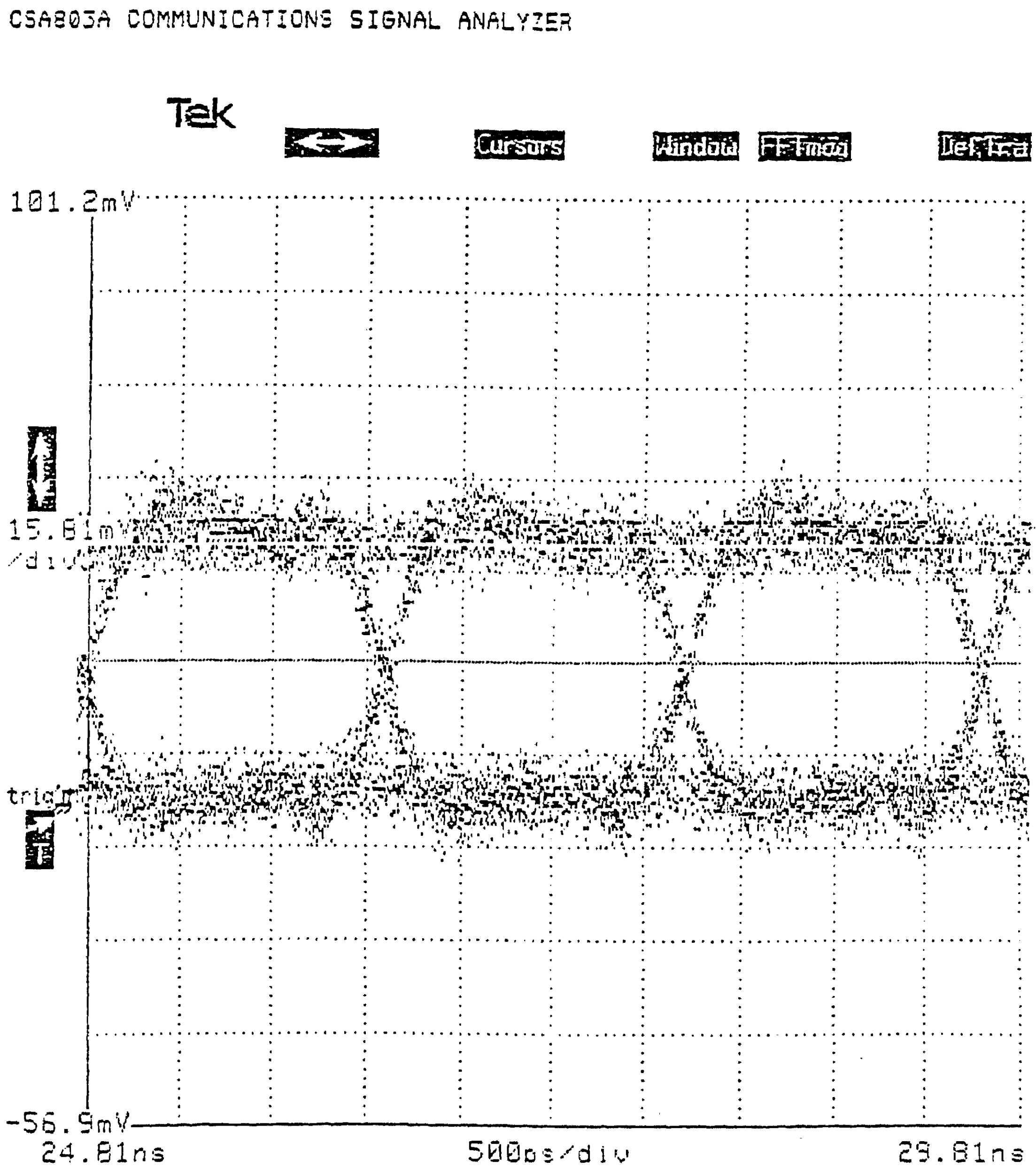

Figure A.10 Eye Diagram After 30 Days 25°C (5.0 Volts)

REFERENCES

1 R. Bayruns, T. Laverick, and N. Scheinberg, "Design of low noise wide dynamic range GaAs optical preamps," presented at the IEEE Int. Conf. Circuits Syst., Singapore, June 1991.

2 A. Abidi, "Gigahertz transresistance amplifiers in fine line NMOS," *IEEE Journal Solid- State Circuits,* Vol. SC-19, December 1984.

3 R. Bayruns, "Amplifier having low noise GaAs MESFET load," U.S. patent 07/554,802.

4 R. G. Smith and S. D. Personick, Chapter 4. "Receiver Design for Optical Fiber Communication Systems," *Topics in Applied Physics, Semiconductor Devices for Optical Communications*, Vol.39, Germany: Springer-Verlag, 1987.

5 R.J. Hoss, "Fiber optic communications design handbook," Englewood Cliffs, N.J.: Prentice-Hall, 1990.

6 N. Scheinberg, "High-speed GaAs operational amplifier," *IEEE Journal of Solid-State Circuits, Vol. SC-22*, No. 4, August 1987.

7 S. D. Personick, "Receiver design for digital fiber optic communication systems," *Bell Syst. Tech. J.,* Vol. 52, No. 6, pp. 843-886, July-August 1973.

8 S. D. Personick, P. Balaban, J. Bosbin, and P. Kumer, "A detailed comparison of four approaches to the calculation of the sensitivity of optical fiber system receivers," *IEEE Trans. Commun.*, Vol. COM-25, pp. 541-548, May 1977.

9 G. Keiser, "Optical fiber communications," 2nd ed., New York: McGraw-Hill, 1991.

10 N. Scheinberg, R. Bayruns, P. Wallace, and R. Goyal, "An accurate MESFET model for linear and microwave circuit design," *IEEE Journal of Solid-State Circuits,* Vol. 24, No. 2, April 1989.

11 R. G. Meyer and R. A. Blauschild,"A wide-band low-noise monolithic transimpedance amplifier," *IEEE Journal of Solid-State Circuits,* Vol. 21, No. 4, pp. 530-537, August 1986.

12 K. Ogawa et al., "Noise caused by GaAs MESFETs in optical receivers," *Ibell Syst. Tech. J.,* Vol. 60, pp. 923-928, July-August 1981.

13 J.C. Palais " Fiber optic communications," 3rd ed., Englewood Cliffs, N.J.: Prentice-Hall, 1992.

14 D. R. Smith and I. Garrett, "A simplified approach to digital optical receiver design." *Opt. Quantum Electron.*, Vol. 10, pp. 211-221, 1978.

15 M. N. Sibley and R. Unwin, "Transimpedance optical preamplifier having a common-collector front end," *Electron. Lett.*, Vol. 18, pp. 985-986, 1982.

16 B. Wilson and I. Darwazeh, "Transimpedance optical preamplifier with a very low input resistance," *Electron. Lett.*, Vol. 23, pp. 88-89, 1987.

17 S. Taylor and T. Thomas, "A 2pA/√Hz GaAs MESFET transimpedance amplifier," presented at IEEE Inter. Solid-State Circuits Conference, San Jose, February 1994.

18 F. Capasso, "Band-gap engineering: from physics and materials to new semiconductor devices," *Science 235.*, pp. 172-176, January 1987.

19 J.L. Hullett and T.V. Muoi, " A feedback receive amplifier for optical transmission systems," *IEEE Trans. Commun.*, Vol. COM 24, pp. 1180-1185, October 1976.

20 K. Ogawa and B. Owen, "Long wavelength optical receiver using a short channel Si MOSFET," *Tech. Dig. Conf. Laser & Electro Optics* (CLEO) (Washington D.C.), pp. 56-57, June 1981.

21 "Synchronous Optical Network (SONET) transport systems: Common generic criteria," Bellcore, Tech. Advisory TA-NWT-000253, Issue 6, September 1990.